의학박사 학위논문

Distribution of *LGR5*$^{+}$ cells and associated implications during the gastric tumorigenesis

위암 발달 단계에서 *LGR5* 양성 줄기세포의 분포와 의미 연구

2015 년 2 월

서울대학교 대학원

의학과 병리학전공

장 보 근

A thesis of the Degree of Doctor of Philosophy

위암 발달 단계에서 *LGR5* 양성 줄기세포의 분포와 의미 연구

Distribution of *LGR5*$^{+}$ cells and associated implications during the gastric tumorigenesis

February 2015

The Department of Pathology,

Seoul National University

College of Medicine

Bo Gun Jang

Distribution of *LGR5*$^{+}$ cells and associated implications during the gastric tumorigenesis

by
Bo Gun Jang

A thesis submitted to the Department of Pathology in partial fulfillment of the requirements for the Degree of Doctor of Philosophy in Pathology at Seoul National University College of Medicine

February 2015

Approved by Thesis Committee:

Professor _____ **Chairman**
Professor _____ **Vice chairman**
Professor _____
Professor _____
Professor _____

ABSTRACT

Lgr5 was identified as a promising gastrointestinal tract stem cell marker in mice, and lineage tracing experiments demonstrated that *Lgr5*$^+$ cells may not only be the cells responsible for the origin of tumors; they may also be the so-called cancer stem cells. In the present study, we investigated the presence of *LGR5*$^+$ cells and their biological significance in normal human gastric mucosa and gastric tumors. RNAscope, a newly developed RNA *in situ* hybridization technique, specifically labeled *LGR5*$^+$ cells at the basal glands of the gastric antrum. Notably, the number of *LGR5*$^+$ cells remarkably increased in intestinal metaplasia (IM). In total, 76% of gastric adenomas (GAs) and 43% of early gastric carcinomas were positive for *LGR5*. *LGR5*$^+$ cells were found more frequently in low-grade tumors with active Wnt signaling and an intestinal gland type, suggesting that *LGR5* is likely involved in the very early stages of Wnt-driven tumorigenesis in the stomach. Interestingly, similar to stem cells in normal tissues, *LGR5*$^+$ cells were often restricted to the base of the tumor glands, and such *LGR5*$^+$ restriction was associated with high levels of intestinal stem cell markers such as *EPHB2*, *OLFM4*, and *ASCL2* supporting the idea that *LGR5*$^+$ cells may act as stem cells in GAs. In addition, we found that *LGR5* positivity is associated with worse clinical outcomes for the gastric cancer patients with nuclear β-catenin expression. However, induced *LGR5* overexpression showed no survival benefit in the gastric cancer cell lines. In conclusion, *LGR5* positive cells are present at the base of gastric antrum of human, and their population dramatically expands in IM. Most gastric

adenomas contain a large number of *LGR5*-expressing cells, which tend to locate at the base of tumor glands co-expressing other intestinal stem cell markers, suggesting the possibility of *LGR5* functioning as tumor stem cells in human gastric adenomas.

Keywords: Leucine-rich repeat-containing G-coupled Receptor 5 (*LGR5*), cancer stem cell, gastric tumorigenesis

Student number: 2009-30581

CONTENTS

LIST OF TABLES

LIST OF FIGURES

INTRODUCTION

Cancer stem cell theory has drawn considerable attention since it was first demonstrated in hematologic malignancies. A growing body of evidence from studies of various solid tumors also supports the concept (1). Because cancer stem cells (CSCs) are believed to be the only tumor cell subpopulation with the potential to establish an entire tumor, especially after chemoradiation therapy, CSC targeting may be a novel approach through which to improve patient outcome (2).

Although many proteins have been proposed as markers of cancer stem cells, the identification and confirmation of such markers in normal human tissues remains challenging. In the gastrointestinal tract, a number of putative stem cell markers such as *Lgr5* (3), *Bmi-1* (4), and *Prominin-1* (5) have been identified. Among these, *Lgr5* (Leucine-rich repeat containing G-protein-coupled receptor 5) is the most promising and established marker. Lineage tracing techniques have clearly shown that *Lgr5* is an adult stem cell marker expressed in the small intestine, colon, stomach, and hair follicles in mice (3). Apc-mutant *Lgr5* cells were reported to be the origin of progressively growing adenomas (6). Additionally, $Lgr5^{+}$ cells were found to be the multipotent tumor stem cells that produced all other adenoma cell types in intestinal adenomas (7). *Lgr5* seems to be the first reported biomarker for stem cells in both normal intestinal mucosa and corresponding tumor tissues.

For several decades, the isthmus region of the stomach has been widely accepted as a stem cell reservoir, based on indirect evidence such as a high proliferative activity and the presence of immature granule-free cells that resemble embryonic stem cells (8). However, in vivo lineage tracing revealed that a group of *Lgr5*$^{+}$ cells at the base of the pyloric glands were multipotent stem cells that contributed to daily epithelial renewal (9). The Wnt-driven tumor initiation induced by targeted ablation of Apc tumor suppressor activity was also suspected to occur in the stomach *Lgr5*$^{+}$ cells. (9).

Despite those remarkable discoveries pertaining to *Lgr5* as an adult stem cell marker in mice, the relevance of *LGR5*expression in human tissues has not been fully evaluated. This is largely because the *in vivo* lineage tracing experiments, which was used in mice to demonstrate the stem cell activity of candidate cells, cannot be applied to stem cell research in humans (8). Although several studies have attempted to determine the presence of *LGR5*$^{+}$ cells either with antibodies (10-13) or with RNA in situ hybridization (ISH) (14, 15), none of the studies provided convincing evidence supporting the presence of *LGR5*$^{+}$ cells in human tissues. Indeed, the lack of a reliable antibody to *LGR5* is the main obstacle in identifying human counterparts of mouse *LGR5*$^{+}$ cells for use in clinical applications.

In this study, using advanced RNA in situ hybridization technique, we investigated the expression of *LGR5* over the gastric tumorigenesis. We revealed that *LGR5*$^{+}$ cells are located at the base of the antral glands in the

human stomach and that this cell population is remarkably expanded in intestinal metaplasia (IM). We also discovered most gastric adenomas (GAs) to contain a large number of *LGR5*-expressing tumor cells that often reside at the basal areas of tumor glands in a similar manner to *LGR5*$^{+}$ cells in the intestinal mucosa, and the lower halves of GA glands, which harbor most of the *LGR5*$^{+}$ cells, specifically coexpress intestinal stem cell markers such as EPHB2, OLFM4, and ASCL2. These findings suggest that *LGR5* is a tumor stem cell marker during the early stage of intestinal-type gastric tumorigenesis.

MATERIALS AND METHODS

1. Subjects

We analyzed formalin-fixed and paraffin-embedded (FFPE) gastric tumors collected from 840 gastrectomy specimens from 2004 to 2005 and 159 patients who underwent endoscopic submucosal dissection (ESD) from 2008 to 2010 at Seoul National University Hospital, Seoul, Korea. Clinico-pathological data such as patient age and gender, histological tumor type, Lauren's classification, and evidence of lymphatic invasion were obtained by reviewing the medical charts and pathological records. Gastric biopsy tissues were obtained from the five children under the age of 10 years who undergone endoscopic examination due to chronic abdominal pain. A normal human skin specimen including hair follicles was obtained from a patient with basal cell carcinoma, and normal small and large intestine samples, which were confirmed to be non-cancerous tissues by histopathological analyses, were obtained from a patient with colon cancer. Unfixed, fresh-frozen, gastric cancer tissues and non-tumorous gastric mucosa were available from 35 patients who underwent gastrectomy from 2001 to 2005 at Seoul National University Hospital.

2. Cell lines and cultures

Fifteen gastric cancer cell lines (SNU1, SNU5, SNU16, SNU216, SNU484, SNU601, SNU620, SNU638, SNU668, SNU79, MKN1, MKN28, MKN45, MKN74 and AGS) used in the study were obtained from the Korean Cell Line

Bank (http:cell-bank.snu.ac.kr, Seoul, Korea) and maintained in RPMI-1640 (JBI, Seoul, Korea) supplanted with 10% fetal bovine serum (Hyclone, Logan, UT), 100 units/ml penicillin and 100 μg/ml streptomycin (Sigma Aldrich, St. Louis, MO, USA). Cells were incubated at 37℃ in a humidified atmosphere with 5% CO_2.

3. Tissue microarray (TMA) construction

Core tissue biopsies (2 mm in diameter) were obtained from individual FFPE gastric tumors (donor blocks) and arranged in a new recipient paraffin block (tissue array block) using a trephine apparatus (SuperBioChips Laboratories, Seoul, Korea). 14 TMAs containing 840 gastric cancers from gastrectomy specimens were generated, and three TMAs were produced containing 53 gastric tumors that had been removed by ESD, and 7 normal non-tumorous gastric mucosa samples, including the antral glands, fundic glands, and IM. An additional TMA, comprising 30 active gastritis cases, was constructed from the specimens of the patients with gastric tumors.

4. RNA in situ hybridization (ISH)

ISH for *LGR5*, *EPHB2*, *ASCL2*, *OLFM4*, and *CDX2* was performed with the RNAscope FFPE assay kit (Advanced Cell Diagnostics, Inc., Hayward, CA) according to the manufacturer's instructions. Briefly, 4μm formalin-fixed, paraffin-embedded tissue sections or TMA sections were pretreated with heat and protease digestion and then hybridized with a target probe for *LGR5*. Thereafter, an HRP-based signal amplification system was hybridized to the

target probe before color development with 3,3′-diaminobenzeidine tetrahydrochloride (DAB). Positive staining was defined as the presence of brown punctate dots in the nucleus and/or cytoplasm. The housekeeping gene ubiquitin C (UBC) served as a positive control. The DapB gene, which is derived from a bacterial gene sequence, was used as a negative control. For gastric tumors, *LGR5* staining was scored based on the percentage of tumor cells expressing *LGR5* as follows: score 0, absence of *LGR5*$^+$ tumor cells; score 1, 1%–5% of *LGR5*$^+$ tumor cells; score 2, 6%–25% of *LGR5*$^+$ tumor cells; and score 3, 26%–100% of *LGR5*$^+$ tumor cells. The results were grouped as positive (score 2 or 3) or negative (score 0 or 1), given that normal gastric mucosa was identified as score 1 for *LGR5* expression.

5. Immunohistochemistry

Immunohistochemistry was performed on 4μm TMA sections using a BOND-MAX automated immunostainer and a Bond Polymer Refine Detection kit (Leica Microsystems, Wetzlar, Germany) according to the manufacturer's instructions. The Ventana BenchMark XT automated staining system (Ventana Medical Systems, Tucson, AZ) was only used for claudin-18 staining. The primary antibodies used were anti-β-catenin (Novocastra Laboratories Ltd., Newcastle, UK; 17C2; 1:800), anti-CD10 (Novocastra; 56C6; 1:100), anti-CDX2 (BioGenex, San Ramon, CA; CDX2-88; 1:500), anti-MUC2 (Novocastra; Ccp58; 1:300), anti-MUC5AC (Novocastra; CLH2; 1:300), anti-MUC6 (Novocastra; CLH5; 1:100), and anti-claudin-18 (Invitrogen, Carlsbad, CA; 34H14L15; 1:1000) antibodies. Nuclear β-catenin staining was

considered positive when more than 10% of the tumor cell nuclei were strongly stained for β-catenin. MUC5AC is expressed in foveolar cells in the stomach, and MUC6 is expressed in mucous cells in the neck of the oxyntic mucosa or in the pyloric glands. MUC2 is expressed in goblet cells with IM in the stomach. CD10 glycoprotein is expressed on the brush borders of intestinal epithelial cells. MUC5AC and MUC6 are gastric phenotypic markers, and MUC2 and CD10 are intestinal phenotypic markers (16). Based on the phenotypic combinations of mucin expression, gastric tumors were classified into the following 4 groups: combined, gastric, intestinal, and unclassified (17).

6. Laser-capture microdissection and RNA extraction

For each patient, the upper and lower portions of the tumor glands and the normal gastric and intestinal mucosa were isolated from 5 to 6 sections. Briefly, 4μm paraffin-embedded tissue sections were obtained, and the areas of interest were selectively microdissected using a laser microdissection device (ION LMD, Jung Woo International Co., Seoul, Korea) without deparaffinization or staining procedures in order to minimize further cellular RNA damage. Total RNA was extracted from the laser-captured areas with an RNeasy FFPE Kit (Qiagen, Valencia, CA) according to manufacturer's instructions, with a slight modification involving extended proteinase K digestion for at least 17 hours after the deparaffinization step (18).

7. Quantitative real-time PCR

cDNA was prepared from 0.5–1μg of total RNA with oligo dT or random hexamer primers and the GoScript reverse transcription system (Promega, Madison, WI). PCR reactions were performed with Premix EX Taq (Takara Bio, Shiga, Japan) according to the manufacturer's recommendations and with the following cycling conditions: initial denaturation for 30 s at 95℃, followed by 40–50 cycles of 95℃ for 5 s and 60℃ for 34 s, in an Applied Biosystems 7500 Real-Time PCR System (Applied Biosystems, Foster City, CA). The data were analyzed using the 7500 system SDS software program (v1.4; Applied Biosystems). The following TaqMan gene expression assays were used: Hs00173908_m1 (*LGR4*), Hs00173664_m1 (*LGR5*), Hs00663887_m1 (*LGR6*), Hs00362096_m1 (*EPHB2*), Hs00270888_s1 (*ASCL2*), Hs00197437_m1 (*OLFM4*), Hs01009250_m1 (*PROM1*), Hs010780810_m1 (*CDX2*), Hs00212584_m1 (*CLDN18*), and Hs0275899_g1 (*GAPDH*). GAPDH served as the endogenous control. The relative quantification of the mRNA was calculated using the comparative threshold cycle (Ct) method. All experiments were performed in duplicate.

8. Transfection

Full-length cDNA encoding *LGR5* (pEX-LGR5) was purchased from GeneCopoeia (Rockville, MD, USA). Cells were seeded at 1 x 10^6 cells/well in 6-well plate and transfected with 2.5 μg of pEX-LGR5 or control vector (pEX-EGFP) using Lipofectamine 2000 transfection reagent (Invitrogen, CA, USA) according to manufacturer's instructions. One day

after transfection, cells were subjected to RT-PCR, western blot, and proliferation assay.

9. Western blot analysis

Cellular proteins were extracted from the gastric cancer cells in lysis buffer (iNtRON Biotechnology, Seongnam, Korea), and protein levels were determined by BCA protein assay kits (Pierce, Rockford, IL, USA). The rabbit anti- LGR5 and mouse anti-β-actin (Sigma Aldrich) were used as primary antibodies. After overnight incubation at 4℃ and washing with TBS containing 0.1% Tween-20, blots were incubated for 1 hr at room temperature with secondary antibodies, washed and visualized using ECL kits (Pierce).

10. Proliferation assay

24 hours after transfection in 6-well plate, cells were harvested and seeded at 5 x 10^3 cells /well on 96-well plates and incubated at 37℃. Recombinant RSPO1 (R-Spondin 1) (R&D systems, Minneapolis, MN) was added at a concentration of 500ng/ml. After adding 10μl of Cell Counting Kit-8 reagent (Dojindo, Tokyo, Japan) into each well and incubating for 1 hour, absorbance was measured at 450nm using a spectrophotometer (Thermo Labsystems, Beverly, MA, USA).

11. Wound healing assay

AGS and SNU484 cells were cultured in 6-well plates until confluent after transfection of control vector or *LGR5*. The monolayer was scratched with a

pipette tip to create a wound and washed twice with culture media to remove cell debris. Cellular migration was monitored and photographed at 0 and 48 h respectively.

11. Statistical analysis

Statistical analyses were performed using the PASW 18.0 statistical software program (IBM SPSS Statistics, Chicago, IL, USA) and Prism version 5.0 (GraphPad Software, Inc., San Diego, CA, USA). The correlations between *LGR5* positivity and clinico-pathological parameters were tested using the λ^2-test or Fisher's exact test. Between-group comparisons of the real-time PCR data were performed using Student's t-test. The significance of the relationship between *LGR5* and *CD133* expression was assessed with the Pearson correlation test. The correlation between the scores according to RNA ISH and the *LGR5* transcripts measured by RT-PCR was evaluated by the Spearman correlation test. Survival curves were estimated using Kaplan-Meier method, and the significances of differences between survival curves were determined using log-rank test. The results were considered significant when $p < 0.05$.

11. Ethical Statement

All human specimens were obtained from curative surgery after informed consent was obtained according to institutional regulations. The study was approved by the Institutional Review Board of Seoul National University Hospital (reference: H-1209-037-424).

RESULTS

RNAscope specifically identifies *LGR5*$^+$ stem cells in human tissues.

LGR5$^+$ cells have been well documented in the stem cell niches of knock-in mouse models, including the crypt bases of the small and large intestines and hair follicle bulges (3, 19). However, the identification of *LGR5*$^+$ cells in human clinical specimens has not been very successful, possibly because the sensitivities and specificities of *LGR5* antibodies and RNA ISH techniques are insufficient. In the present study, we applied RNAscope, a novel RNA ISH technology, to examine human FFPE tissues (20). To validate this method before investigating the distribution of *LGR5*$^+$ cells in the stomach, we assessed whether RNAscope could specifically mark *LGR5*$^+$ cells in well-established niches. As expected, groups of *LGR5*$^+$ cells were detected at the exact intestinal and hair follicular locations that had been observed in mice. Almost every small intestinal crypt harbored several *LGR5*$^+$ cells in the basal area (Fig. 1A), and *LGR5*$^+$ cells were interspersed with Paneth cells (Fig. 1B). Most colon crypts contained *LGR5*$^+$ cells, even though the *LGR5* staining intensities were a little weaker than in the small intestine (Fig. 1C, D). Many *LGR5*$^+$ cells were spread along the hair follicle bulges and bulbs (Fig. 1E, F). We also confirmed *LGR5* expression in tumors that arose from these tissues, such as basal cell carcinoma (Fig. 2A) and colonic adenoma (Fig. 2B), as reported in previous studies (15, 21). These findings demonstrated the ability of RNAscope to specifically identify *LGR5*$^+$ stem cells in human FFPE

specimens. To further establish the robustness of RNAscope, we showed that CDX2-expressing tumor cells were positively stained by RNAscope while CDX2-negative adjacent normal gastric epithelial cells were not (Fig. 3).

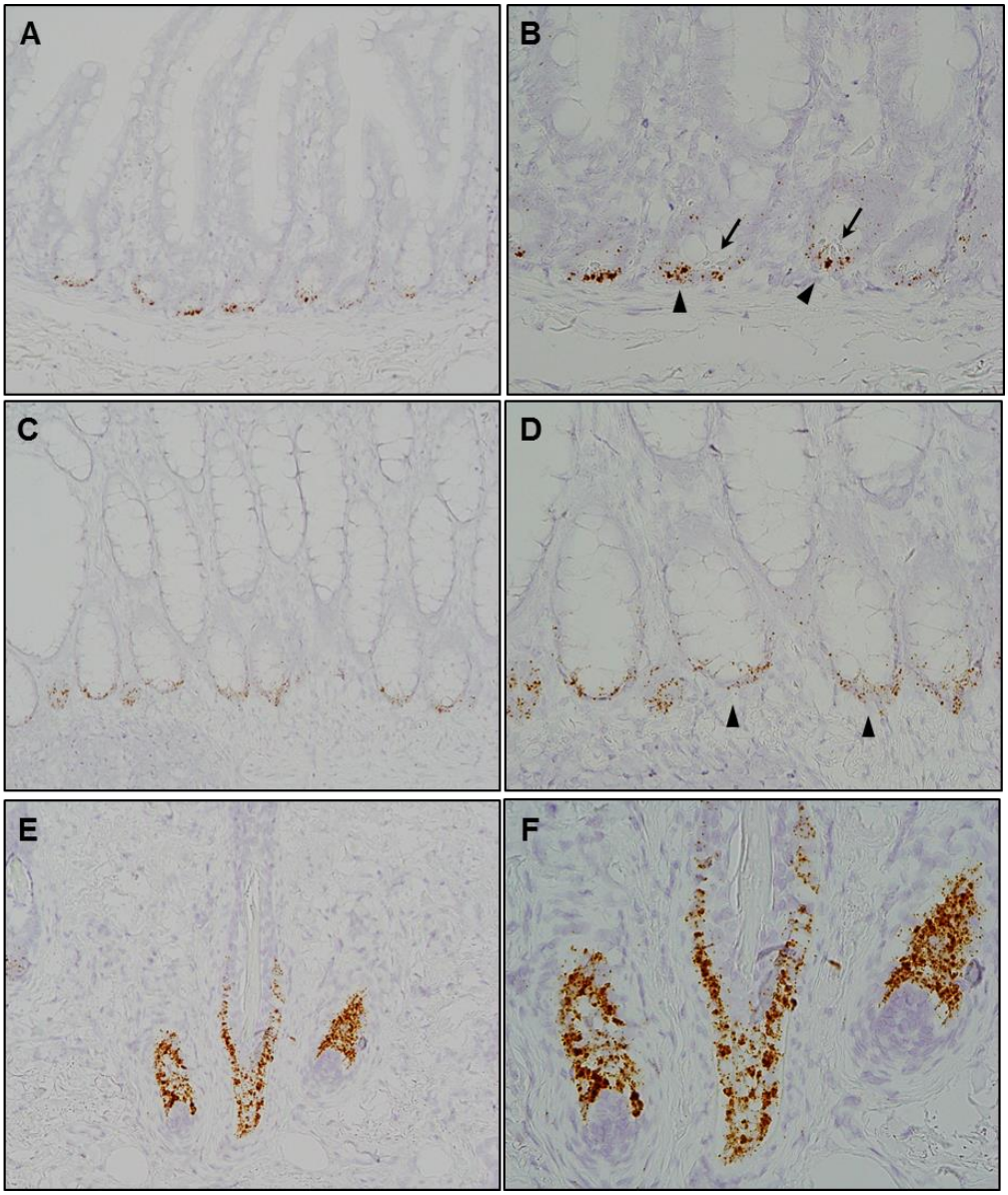

Figure 1. Validation of RNA in situ hybridization (ISH) for the identification of *LGR5*$^{+}$ cells in established niches in normal human tissues. RNA ISH was performed to detect *LGR5*-expressing cells in formalin-fixed and paraffin-embedded small intestine, colon, and hair follicle samples. *LGR5*$^{+}$ cells are indicated by the brown colored dots. (A) *LGR5*$^{+}$

cells were observed at the base of all small bowel crypts. (B) *LGR5*$^{+}$ cells, indicated by arrowheads, were located next to or between Paneth cells, which are distinguished by their characteristic cytoplasmic granules and marked by arrows. (C, D) *LGR5*+ cells indicated by arrow heads reside at the bottom of the crypts in the same way as the small intestine. (E, F) Many *LGR5*$^{+}$ cells were noted in the hair follicle bulges. Magnifications: A, C, E, ×200; B, D,F ×400.

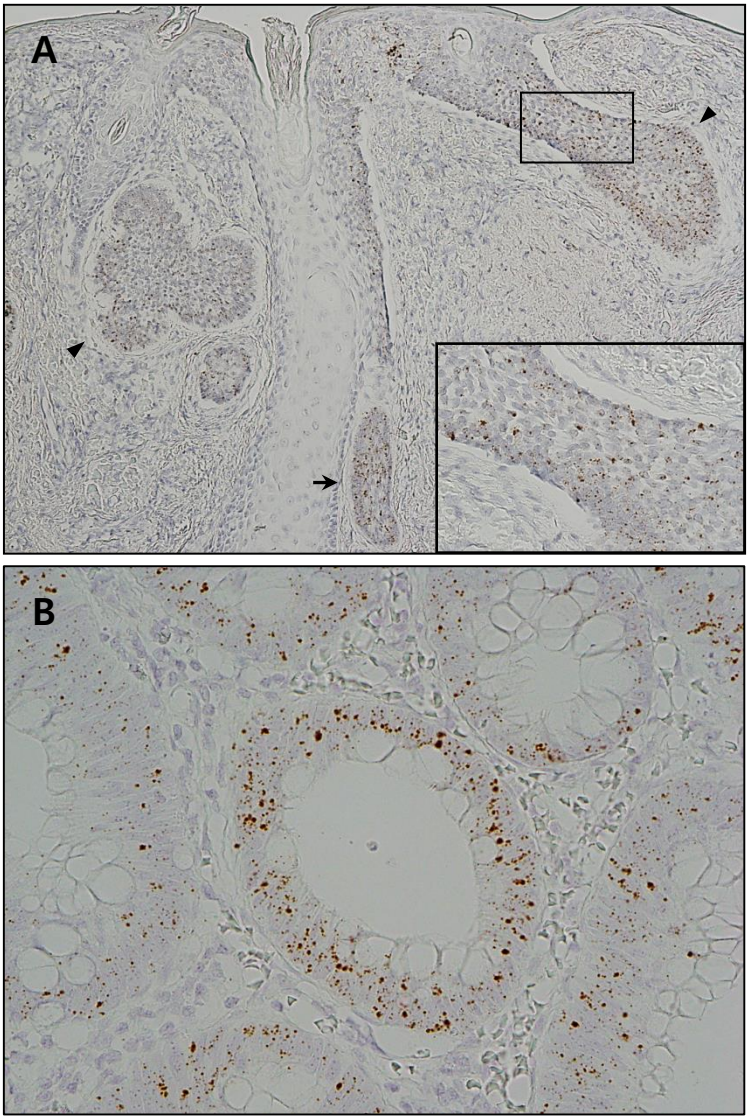

Figure 2. *LGR5* $^{+}$ cells in the basal cell carcinoma of skin and adenoma of colon. (A) *LGR5* stem cells (marked by arrow) are seen at the bulge of hair follicle, and the majority of tumor cells of basal cell carcinoma (indicated by arrow heads) which developed nearby express *LGR5*. Inlet pictures show a representative area at higher magnification. (B) Colonic adenoma cells exhibit *LGR5* expression. Original magnification: A, ×100; B, ×400.

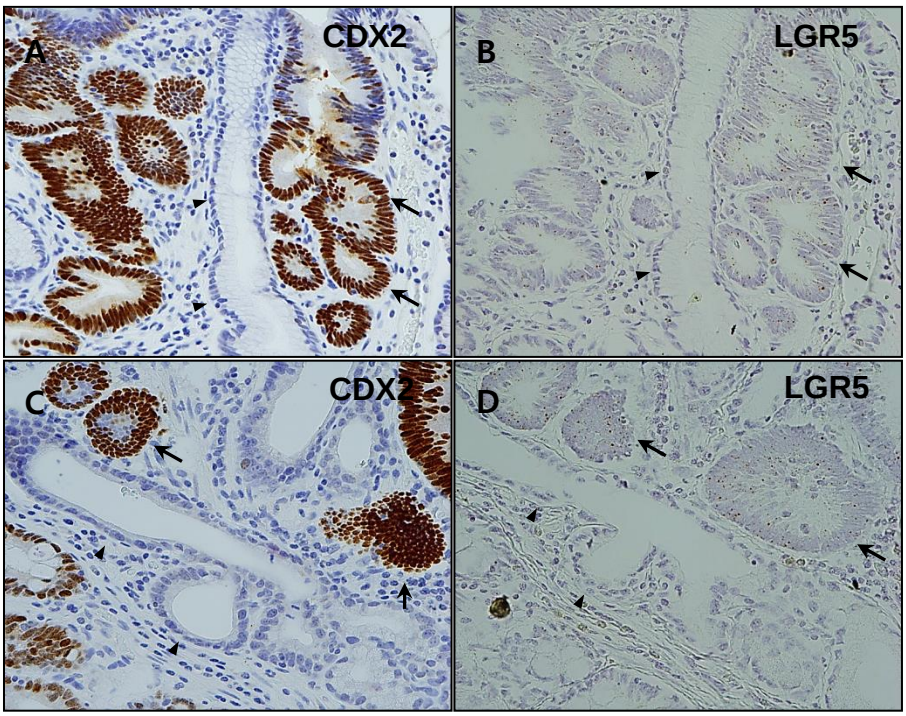

Figure 3. Validation of RNAscope with CDX2 expression in gastric adenomas. CDX2-expressing gastric adenoma cells (indicated by arrows), shown as strong nuclear stain by immunohistochemistry (A and C), are specifically identified by RNAscope (B and D), whereas normal gastric epithelial cells adjacent to tumor cells (indicated by arrow heads), negative for CDX2, do not express *CDX2* transcripts. Original magnification: A, B, C, D ×200.

IM in the stomach is associated with a marked expansion of the *LGR5*$^+$ cell population.

To investigate the spatial distribution of *LGR5*$^+$ cells in the non-tumorous gastric lesions, we examined many different types of gastric mucosa (GM), including gastric mucosa without inflammation or intestinal metaplasia (IM) (n=4 for antrum, n=4 for corpus), GM with active gastritis (n=12), and GM with IM in the antrum (n=5) as well as small bowel (n=5) and colon (n=5). Consistent with the findings from mice, a sparse *LGR5*$^+$ cell population was observed only at the base of the antral glands (Fig. 4A, B), but not at the isthmus or neck region. No *LGR5*$^+$ cells were noted at the fundic glands (Fig. 4C, D), suggesting that *LGR5*$^+$ cells only comprise a small group of stem cells restricted to the antrum. Remarkably, IM was associated with a dramatic increase in the number of *LGR5*$^+$ cells (Fig. 4E, F). Interestingly, *LGR5*$^+$ cells were also detected in IM in the corpus, where no *LGR5*$^+$ cells were present (Fig. 4G, H). *LGR5*$^+$ cells were mostly restricted to the basal areas of the metaplastic glands, similar to the pattern observed in the small intestine. Active gastritis with or without *Helicobacter pylori* infection had no effect on the *LGR5*$^+$ cell population (Fig. 4I). When counting the number of glands with *LGR5*$^+$ cells among 20 consecutive glands in both the gastric and intestinal mucosa, we surprisingly discovered that the frequency of glands with *LGR5*$^+$ cells in IM was almost as high as that in the small intestine (Fig. 4I), indicating that IM of the stomach seems to recapitulate intestinal mucosal features with regard to the stem cell population. Since *LGR5* expression was dramatically induced by metaplastic process and all the specimens we used

were obtained from adults with the history of chronic gastritis, it is possible that those LGR5 cells in normal antral glands might only represent the traces of past history of IM that had disappeared. To exclude this possibility, we collected biopsy samples from children who do not have any evidence of inflammation or *H.pylori* infection and examined the *LGR5* expression in the antral mucosa. Figure 5 shows $LGR5^{+}$ cells at the bottom of antral glands of the children, indicating that $LGR5^{+}$ originally exist in human gastric antrum.

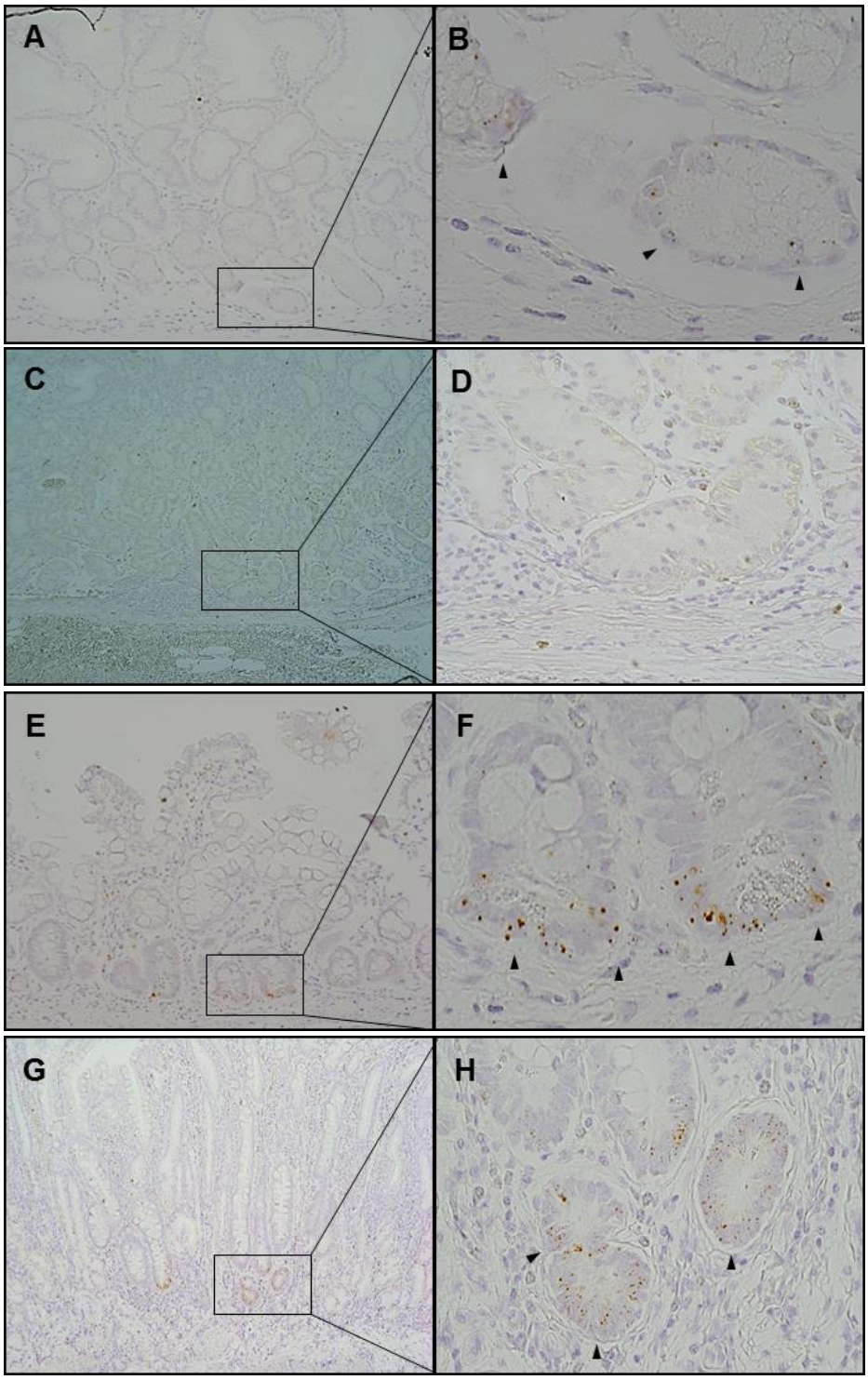
A
B
C
D
E
F
G
H

I

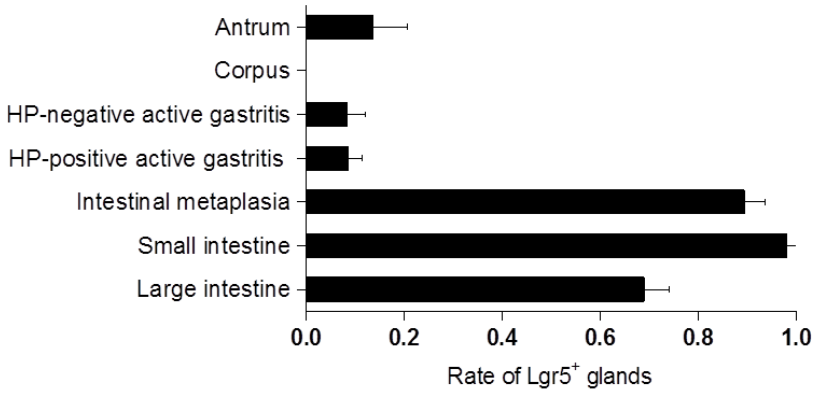

Figure 4. Localization of *LGR5*$^+$ cells in the gastric antrum and intestinal metaplasia. (A, B) Rarely, a few *LGR5*$^+$ cells are observed in the basal region of the gastric antrum. (C, D) No *LGR5*$^+$ cells are noted in the corpus. (E, F) The *LGR5*$^+$ cell population, which is located primarily in the lower regions of glands, dramatically increases in IM of the antral glands. (G, H) Interestingly, IM occurring in the corpus has as many *LGR5*$^+$ cells as the IM in the antrum. Arrows indicate the fundic glands. (E) Study of the ratio of *LGR5*$^+$ cell-containing glands among 20 consecutive glands show that the metaplastic glands have a similar number of *LGR5*$^+$ cells as the small intestine. *LGR5*$^+$ cells are indicated by arrowheads. HP, *Helicobactor pylori*. Original magnifications: A, C, E, G ×100; B,F ×600; D,H ×400.

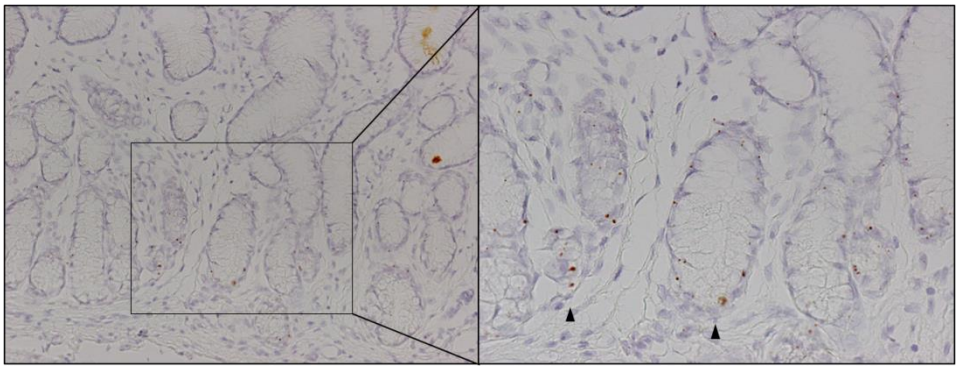

Figure 5. *LGR5*$^{+}$ cells in the gastric antrum of children. Gastric tissues were obtained from the children ranging in age from 6 to 10 through endoscopic examination which found no mucosal abnormalities. RNA ISH revealed LGR5 expressing cells (arrow heads) confined at the bases of antral glands. Original magnifications: A ×200; B×400.

The *LGR5*$^+$ cell population specifically increases with IM and positively correlates with CD133 expression.

To provide further evidence of the close relationship between the appearance of *LGR5*$^+$ cells and IM, we collected 11 fresh-frozen, non-tumorous gastric tissues and divided them into 2 groups according to the *CDX2* expression level, either *CDX2*-low and *CDX2*-high, because *CDX2* is highly expressed in IM of the stomach (22) (Fig. 6A). When *LGR4*, *5*, and *6* expression levels were compared between the 2 groups, only the *LGR5* level was significantly higher in the *CDX2*-high group, thus confirming a specific association between *LGR5* expression and gastric mucosal intestinalization (Fig. 6B, C, and D). The *CD133* expression level was also higher in the *CDX2*-high group, although the difference was not statistically significant (p = 0.055; Fig. 6E), which led us to hypothesize that the increased number of *LGR5*$^+$ cells is associated with *CD133* expression, because *CD133* is a stem cell marker in many different types of tumors (23). Indeed, we found a positive correlation between *LGR5* and *CD133* expression when analyzing the RT-PCR data from the normal gastric mucosa (Pearson correlation coefficient = 0.47, p = 0.02) (Fig. 6F). In a mouse study, *LGR5*$^+$ cells were the cells of origin of a Wnt-driven gastric adenoma (GA) (9). Most human GAs occur from an IM background (24), and most have *APC* gene mutations (25). Based on these findings, we postulated that IM in the stomach enhances the risk of tumor development by increasing the *LGR5*$^+$ cell population, which is highly susceptible to transformation by *APC* mutation.

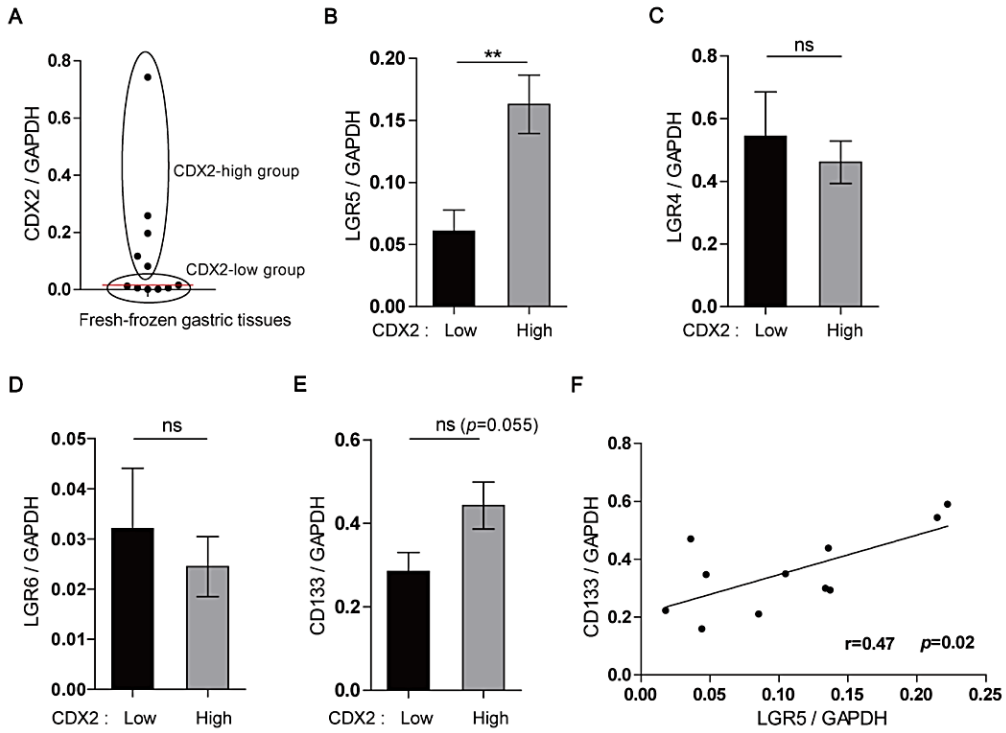

Figure 6. Increased *LGR5* expression with gastric intestinalization. Semi-quantitative real time PCR was performed with fresh-frozen normal gastric tissues (n=11) to analyze the expression of *LGR4*, *LGR5*, *LGR6*, *CDX2*, and *CD133*. (A) The samples were divided into the *CDX2*-high and low groups according to the median *CDX2* value (red line). *LGR5* expression was significantly higher in the *CDX2*-high group (B), whereas there were no differences in the levels of *LGR4* (C) and *LGR6* (D) between the groups. (E) *CD133* expression was higher in the *CDX2*-high group, although this was not statistically significant. (p = 0.055) (F) A positive correlation was observed between *LGR5* and *CD133* expression. (Pearson correlation coefficient = 0.47, p = 0.02)

$LGR5^+$ tumor cells are often confined to the basal area of tumor glands, reminiscent of normal stem cell niches.

To explore the effects of $LGR5^+$ cells on tumor development in the human stomach, we constructed tissue microarrays and examined the expression of *LGR5* in gastric tumors obtained by ESD, including GAs and early gastric carcinomas (EGCs). The *LGR5* expression levels were score d according to the percentage of $LGR5^+$ tumor cells (Fig. 7A, B). Tumors above score 2 were considered positive. To confirm the results from RNA ISH, total RNAs were obtained from FFPE samples of gastric adenomas with each scores, non-tumorous gastric mucosa, and intestinal mucosa, and the *LGR5* transcripts were subsequently measured by semi-quantitative RT-PCR. The *LGR5* transcript levels in IM of the stomach were similar to those in the small intestine (Fig. 7C). The RNA ISH assay scores correlated well with the *LGR5* mRNA levels determined by RT-PCR (Spearman correlation coefficient = 0.96; $p < 0.0001$) (Fig. 7D).The degree and pattern of *LGR5* expression varied between the gastric tumors. The *LGR5*-positive tumors could be roughly divided into 2 types based on the distribution of $LGR5^+$ cells: tumors with basal (Fig. 8A) or diffuse (Fig. 8B) patterns. In the basal pattern tumors, the $LGR5^+$ cells were mostly restricted to the base of the adenoma segment, which was reminiscent of both IM and the normal crypt architecture. More than half of the tumors exhibited a basal accumulation of $LGR5^+$ cells, regardless of the histological progression of the gastric tumors, although the overall frequency of *LGR5* positivity declined over the tumor progression (Fig. 9). This observation led us to speculate that these $LGR5^+$ cells function as tumor stem

cells. In a mouse study, the same tendency of *LGR5*$^{+}$ cells to localize toward the base of the adenoma segment was reported in the intestinal adenomas, and their stem cell-like properties were directly demonstrated by the coexpression of other stem cell markers such as *OLFM4* and *ASCL2*, as well as by stem cell activity (7).

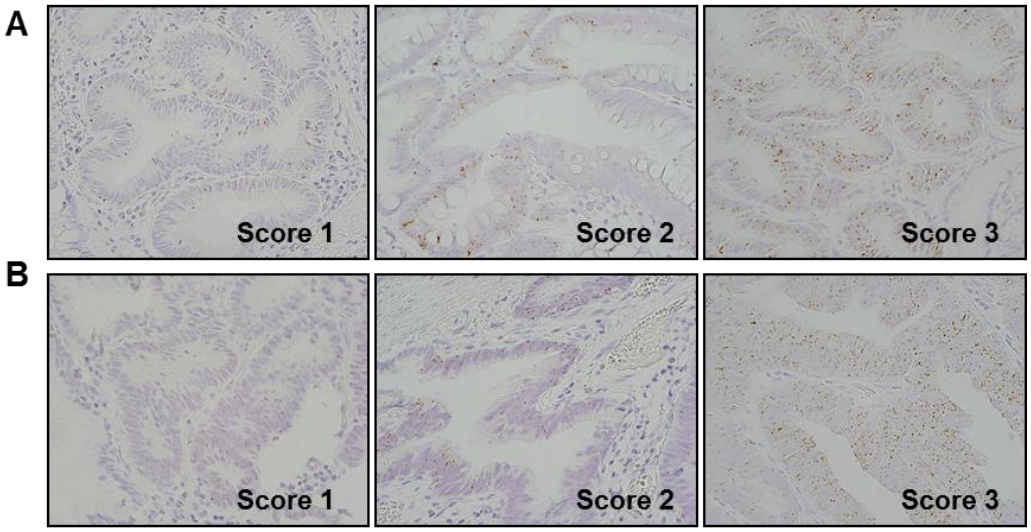
A
Score 1
Score 2
Score 3
B
Score 1
Score 2
Score 3

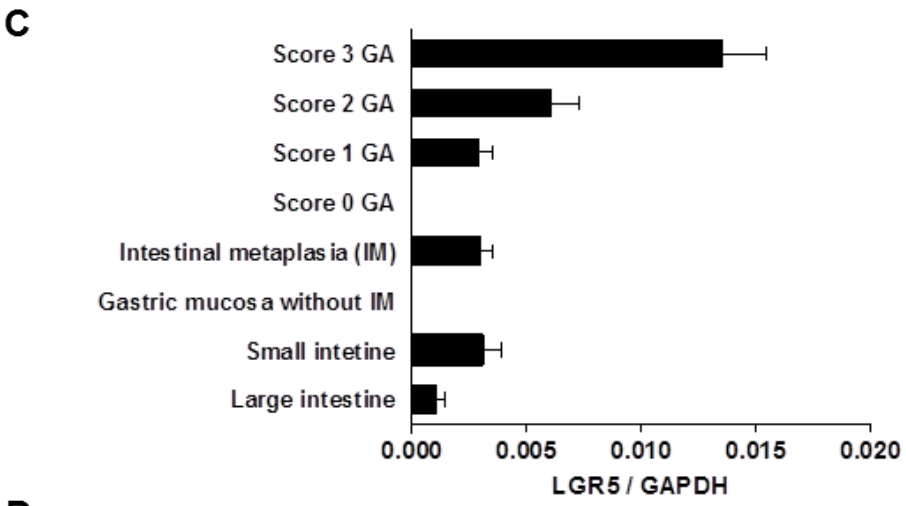
C
Score 3 GA
Score 2 GA
Score 1 GA
Score 0 GA
Intestinal metaplasia (IM)
Gastric mucosa without IM
Small intetine
Large intestine
0.000
0.005
0.010
0.015
0.020
LGR5 / GAPDH

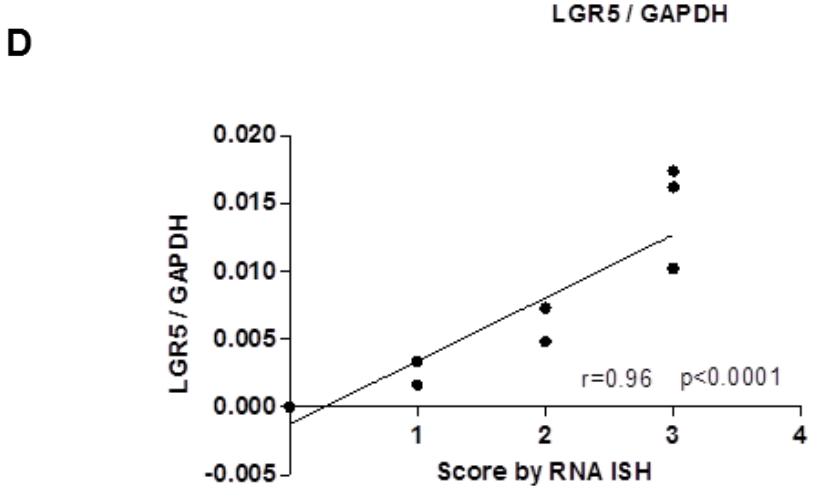
D
0.020
0.015
0.010
0.005
0.000
-0.005
LGR5 / GAPDH
r=0.96 p<0.0001
1
2
3
4
Score by RNA ISH

Figure 7. ***LGR5*-expressing cells in gastric adenomas.** Tissue microarrays were constructed from gastric tumors, including gastric adenomas (GAs) (n=75) and early gastric carcinomas (EGCs) (n=68), that had been removed by endoscopic submucosal dissection. *LGR5* expression in GAs (A) and EGCs (B) was classified according to the percentage of $LGR5^{+}$ tumor cells as scores 0, 1, 2, and 3. (C) Semi-quantitative real time-PCR from GAs (n=11), IM in the antrum (n=3), GM without IM in the corpus (n=4), and small (n=4) and large (n=4) intestinal tissues was performed to confirm the RNA ISH results. (D) There was a positive correlation between the *LGR5* scores in GAs as determined by the RNA ISH and *LGR5* transcripts levels from RT-PCR. (Spearman correlation coefficient = 0.96; $p < 0.0001$) Original magnifications: A, B, ×400.

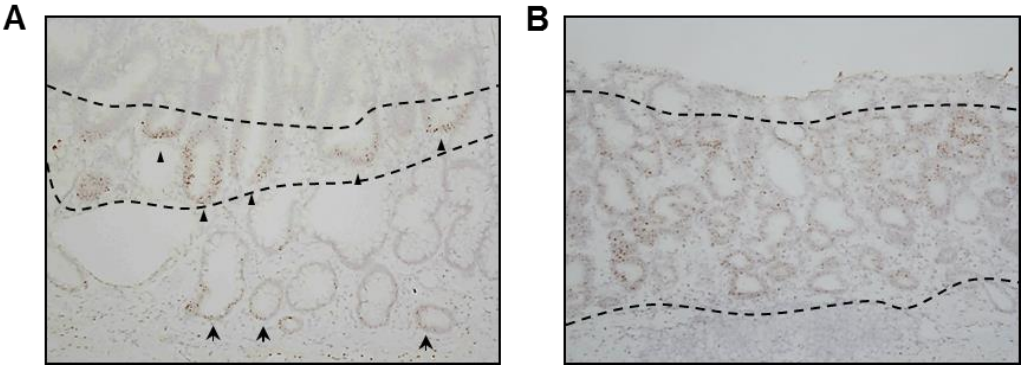

Figure 8. Distribution patterns of *LGR5*$^{+}$ adenoma cells in GAs. (A) Some GAs had a distinct *LGR5*$^{+}$ cell distribution that was restricted to the bases of tumor glands (marked by arrowheads); this distribution was quite similar to that of *LGR5*$^{+}$ cells in IM (indicated by arrows) observed around the tumor. (B) However, some GAs contained *LGR5*-expressing tumor cells in a relatively diffuse distribution pattern. Original magnifications: A, B ×200.

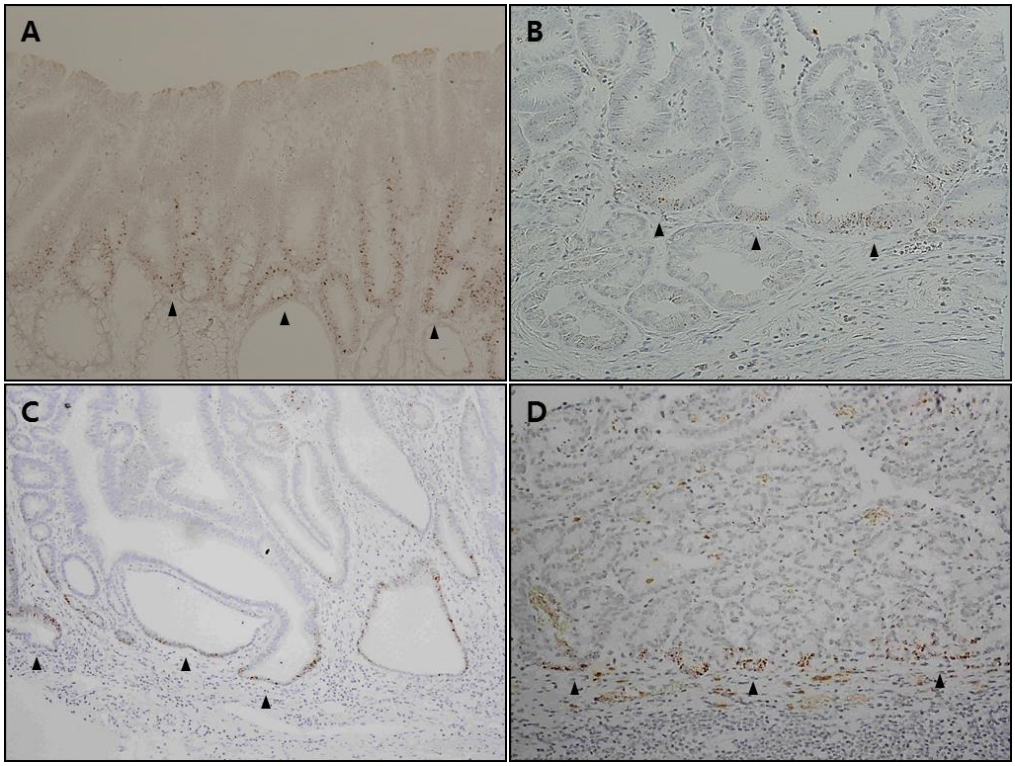
A
B
C
D

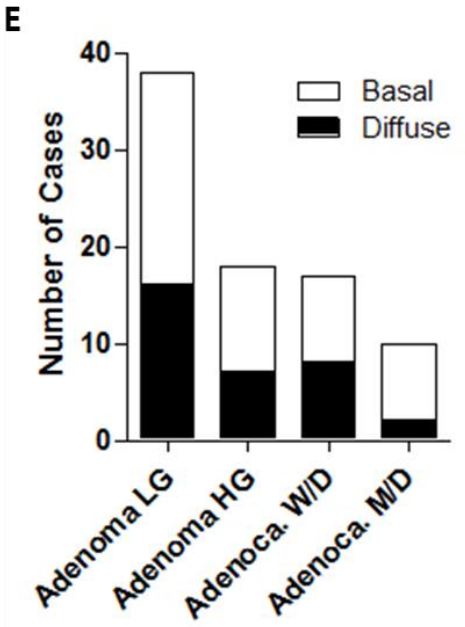
E
Number of Cases
40
30
20
10
0
Basal
Diffuse
Adenoma LG
Adenoma HG
Adenoca. W/D
Adenoca. M/D

Figure 9. Basal arrangement of *LGR5*$^{+}$ cells in gastric tumors. *LGR5* expressing tumor cells are often restricted at the basal part of tumor glands or at the interface between muscularis mucosa and submucosa in the gastric tumors including low grade adenoma (A), high grade adenoma (B), well differentiated adenocarcinoma (C), and moderately differentiated adenocarcinoma (D). (E) Around half of tumors showed basal distribution pattern of *LGR5*$^{+}$ cells regardless of histological type. Original magnification: A, B, D ×200; C ×100.

LGR5 positivity is associated with nuclear β-catenin, histological differentiation, and mucin type in gastric adenomas.

Correlations of *LGR5* positivity with various clinico-pathological factors were evaluated and summarized for GAs (Table 1) and EGCs (Table 2). A total of 57 GA cases (76%) and 31 EGC cases (43%) were positive for *LGR5*. *LGR5* expression was strongly and positively associated with nuclear β-catenin in both GAs (p = 0.015) (Fig. 10A, B) and EGCs (p = 0.000), which was consistent with previous reports that documented a relationship between *LGR5* and Wnt pathway activation (26, 27). *LGR5* expression was higher in low-grade adenomas than in high-grade adenomas (p = 0.025) (Table 1), and the expression tended to decline with tumor dedifferentiation (p = 0.036) (Fig. 10C). Nuclear β-catenin expression also significantly decreased with tumor progression (Table 3). Moreover, *LGR5* expression was higher in adenomas with intestinal-type glands than in those with gastric-type glands (Fig. 10D, E). (p = 0.024). Thus, our findings indicate that *LGR5*$^+$ cells occur more frequently in low-grade tumors with active Wnt pathway signaling and an intestinal gland type, suggesting that *LGR5* is more likely involved in the very early stages of Wnt-driven tumorigenesis in the stomach.

Table 1. Assesment of LGR5 expression in gastric adenomas

	Total (%)	LGR5		*p*-value
		Negative (%)	Positive (%)	
Patients	75 (100)	18 (24)	57 (76)	
Age				
≥65	41 (55)	10 (24)	31 (76)	1.000†
<65	34 (45)	8 (24)	26 (76)	
Gender				
Female	22 (29)	4 (18)	18 (82)	0.560†
Male	53 (71)	14 (26)	39 (74)	
Grade				
Low	47 (63)	7 (15)	17 (85)	0.025†
High	30 (37)	11 (37)	40 (63)	
β-catenin				
Nuclear stain	44 (59)	6 (14)	38 (84)	0.015†
No nuclear stain	31 (41)	12 (39)	19 (61)	
Mucinous type				
Gastric	13 (17)	7 (54)	6 (46)	0.024#
Intestinal	30 (40)	4 (13)	26 (87)	
Mixed	23 (31)	5 (22)	18 (78)	
Unclassified	9 (12)	1 (11)	8 (89)	

†Fisher's exact test. #Pearson Chi-Sqaure

Table 2. Assessment of LGR5 expression in early gastric carcinomas

	Total (%)	LGR5		*p*-value
		Negative (%)	Positive (%)	
Patients	68 (100)	37 (54)	31 (46)	
Age				
≥65	32 (47)	17 (53)	15 (47)	1.000*
<65	36 (53)	48)	16 (42)	
Gender				
Female	14 (21)	11 (79)	3 (21)	0.069*
Male	54 (79)	26 (48)	28 (52)	
Location				
Cardia	3 (4)	1 (33)	2 (67)	
body	30 (44)	13 (43)	17(57)	0.148#
Antrum	35 (52)	23 (66)	12 (34)	
Histological				
Well	29 (43)	10 (36)	19 (64)	
Moderate	30 (44)	19 (63)	11 (37)	
Poor	5 (8)	4 (80)	1 (20)	0.036#
Signet ring cell	3 (3)	3 (100)	0 (0)	
Papillary	1 (2)	1 (100)	0 (0)	
Depth of invasion				
Lamnina propria	12 (18)	9 (75)	3 (25)	0.249#
Muscularis mucosa	26 (38)	12 (46)	14 (54)	
Submucosa	30 (44)	16(53)	14 (47)	
Lymph nodes				
Metastses	9 (13)	4 (44)	5 (56)	0.722*
No metastases	59 (87)	33 (56)	26 (44)	
β-catenin				
Nuclear stain	15 (22)	2 (13)	13 (87)	0.000*
No nuclear stain	53 (78)	35 (66)	18 (34)	
Mucinous type				
Gastric	23 (34)	12 (52)	11 (48)	
Intestinal	15 (22)	7 (47)	8 (53)	0.752#
Mixed	26 (38)	15 (57)	11 (43)	
Unclassified	4 (6)	3 (75)	1 (25)	

*Fisher's exact test. #Pearson Chi-Sqaure

Table 3. LGR5 and nuclear β-catenin with the progression of gastric cancers

		Gastric adenoma		EGC[#]	*p*-value
		Low grade	High grade		
Total (%)		47	28	69	
LGR5	Positive	40 (85)	18 (64)	31 (45)	0.000*
	Negative	7 (15)	10 (36)	38 (55)	
Nuclear β-catenin	Positive	29 (61)	15 (54)	15 (22)	0.000*
	Negative	18 (39)	13 (46)	54 (78)	

[#]EGC, Early gastric carcinoma; *Fisher's exact test

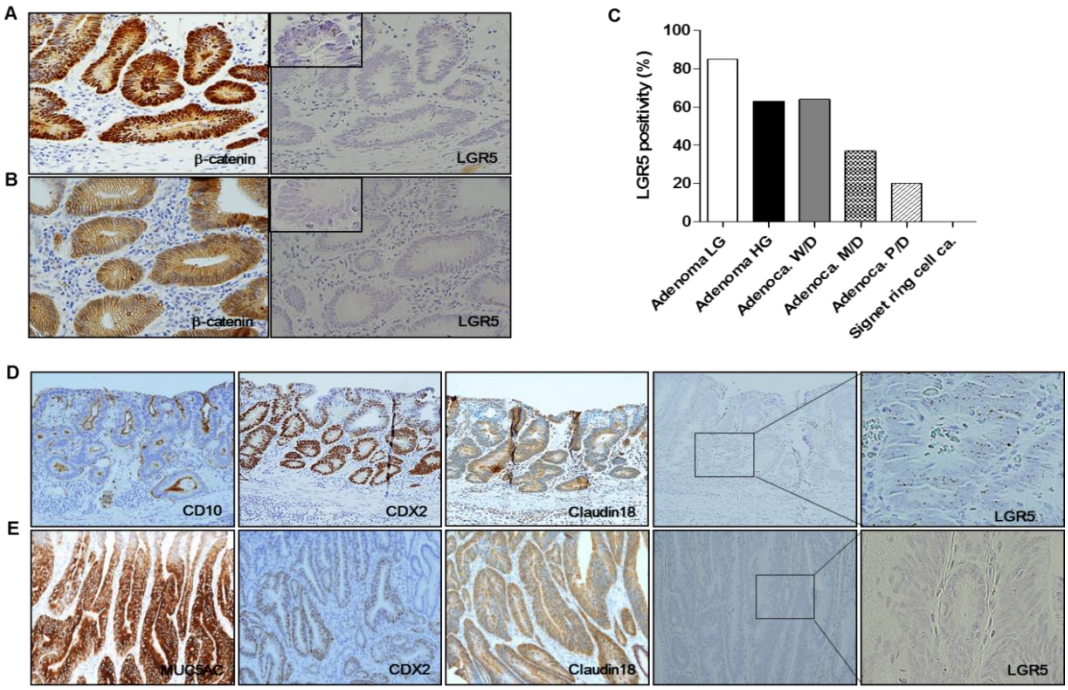

Figure 10. Relationships between *LGR5* positivity and nuclear β-catenin, histological differentiation, and mucinous type in gastric adenomas. Gastric adenomas with strong cytoplasmic and nuclear β-catenin expression (n=44) are highly likely to be positive for *LGR5* (A), whereas adenomas with normal β-catenin expression levels have relatively low *LGR5* positivity (B). (C) As the tumors progress and dedifferentiate, *LGR5* positivity declines. Intestinal-type adenomas (n=30) generally have higher levels of *LGR5* expression (D) than gastric-type adenomas (n=13) (E). CD10 and MUC2 expression refers to the intestinal tumor gland phenotype, and MUC5AC and MUC6 mucin expression represents the gastric gland phenotype. LG, low grade; HG, high grade; Adenoca., adenocarcinoma; W/D, well differentiated; M/D, moderately differentiated; P/D, poorly differentiated. Original magnifications: A, B, D, E, ×200.

LGR5 expression is associated with the levels of other intestinal stem cell (ISC) markers.

The distinct basal restriction of *LGR5*$^+$ cells in some GAs is interesting because it strikingly resembles the restriction of *LGR5*$^+$ stem cells to the niche in normal tissues. To further investigate whether the *LGR5*$^+$ cells in human GAs had any stem cell properties, we analyzed the levels of ISC markers such as *ASCL2*, *EPHB2*, and *OLFM4*, which are highly expressed in stem-like cells from human colorectal cancers (28), as well as in murine intestinal adenomas (7). In general, GAs expressed significantly higher levels of *EPHB2* and *OLFM4* than the non-tumorous gastric mucosa (Fig. 11A). To clarify whether the upregulated expression of ISC markers was related to the *LGR5*$^+$ tumor cells, we microdissected the tumor glands into upper and lower regions (Fig. 11B) and compared the marker transcript levels in both areas. The results confirmed that *LGR5* expression was higher in the lower region, whereas the expression of *LGR4*, which is a close relative of the *LGR5* gene, did not differ between the 2 regions (Fig. 11C). The expression levels of all examined ISC markers were higher in the lower region, where the majority of *LGR5*$^+$ cells exist (Fig. 11C). Furthermore, *CD133* expression was higher in the basal regions of the tumor glands (Fig. 11C). Thus, these findings support the hypothesis that *LGR5*$^+$ cells restricted to the bases of tumor glands retain stem cell properties in human GAs.

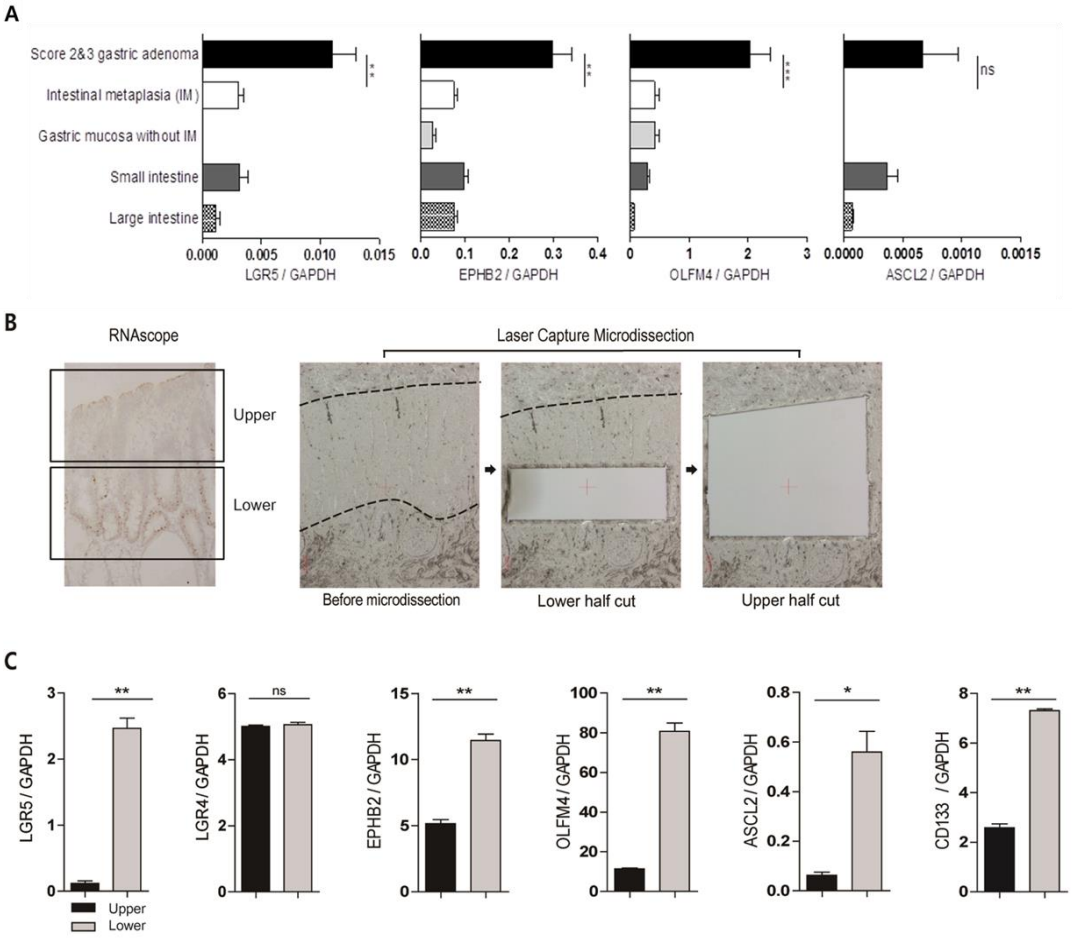

Figure 11. *LGR5*$^{+}$ cells, restricted to the lower regions of tumor glands, are responsible for the high levels of intestinal stem cell (ISC) markers. (A) *LGR5*-positive gastric adenomas (n=8) expressed substantially higher levels of ISC markers such as *EPHB2*, *OLFM4*, and *ASCL2* than non-tumorous gastric mucosa (n=4 for IM, n=4 for GM without IM in the corpus), small (n=3) and large (n=3) intestines, although the difference in *ASCL2* expression was statistically not significant. (B) Lower and upper regions were laser capture microdissected from GAs with basal *LGR5*$^{+}$ cells. (C) Semi-

quantitative real time PCR of the dissected tissues revealed that the basal regions that harbored most *LGR5*$^{+}$ cells had higher levels of ISC markers and *CD133*, whereas no difference in *LGR4* expression was observed between the lower and upper regions.

Basal restriction of *LGR5*$^{+}$ cells in GAs correlates with the differential expression of ISC markers along the gland axes.

To strengthen the hypothesis that the *LGR5*$^{+}$ cells restricted to the bases of tumor glands are essential for the distinct ISC marker expression patterns in the upper and lower regions, we examined a GA with relatively diffuse *LGR5* distribution and a slight basal accentuation of *LGR5* expression. *LGR5* expression in the upper and lower halves of the gland differed little in the adenoma, unlike that in IM and GAs with basal *LGR5* expression (Fig. 12A). Indeed, the wide regional variation in the expression of all ISC markers that was observed in the GAs and IM with basal *LGR5* expression was remarkably reduced in the GA with diffuse *LGR5* expression (Fig. 12B, C, and D). The expression ratios of the lower regions to the upper regions for all ISC markers, including EphB2 (p = 0.018), *OLFM4* (p = 0.002), and *ASCL2* (p = 0.025), were significantly decreased in the GA with diffuse *LGR5* expression, compared to a GA with basal *LGR5* expression (Fig. 12E). These findings indicate that the basal restriction of *LGR5*$^{+}$ cells in GAs is closely correlated with the gradient expression of ISC markers along the gland axes.

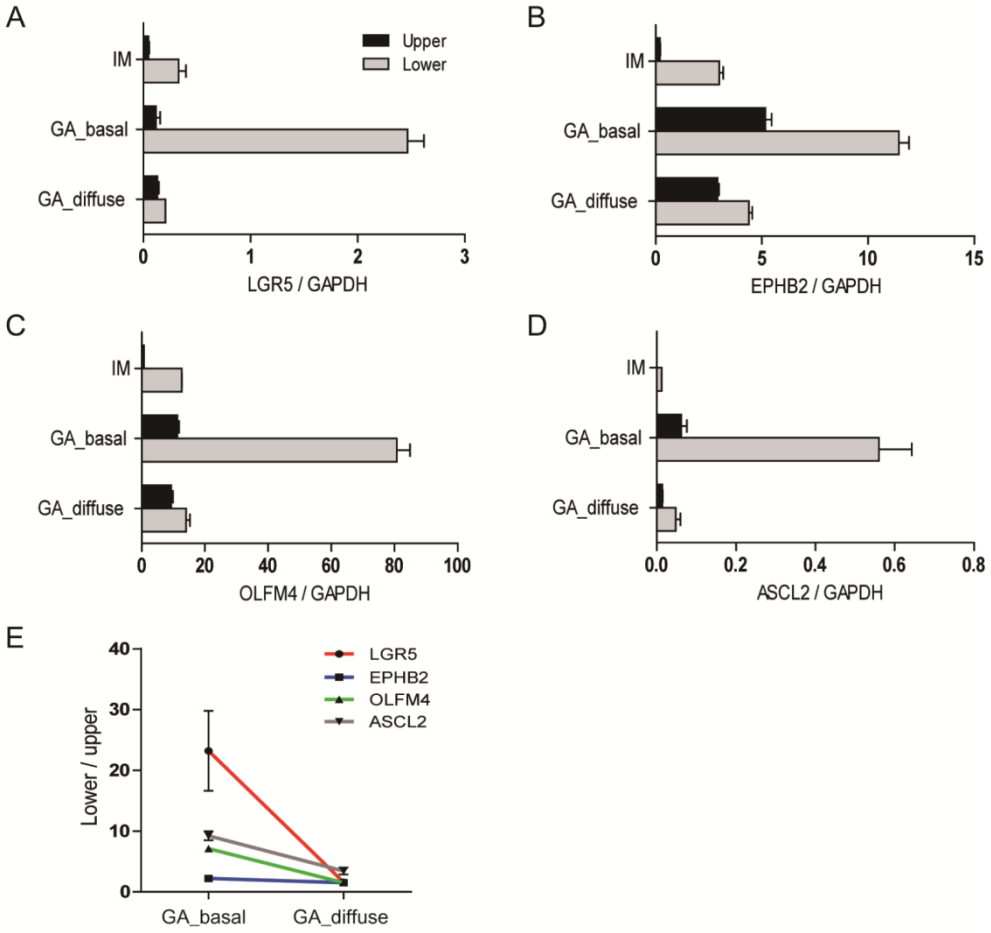

Figure 12. Comparisons of ISC markers expression between gastric adenomas with different *LGR5* distribution patterns. The upper and lower gland regions were selectively microdissected from IM (n=3) and a GA with diffusely distributed *LGR5*$^{+}$ cells (GA_diffuse) to compare the differential expression of ISC markers to those of the GA with basally restricted *LGR5*$^{+}$ cells (GA_basal). RT-PCR analysis of *LGR5* (A), *EPHB2* (B), *OLFM4* (C), and *ASCL2* (D) expression demonstrated that the ISC marker expression gradient between the lower and upper gland regions was remarkably reduced in the GA with diffusely distributed *LGR5*$^{+}$ cells (E).

Spatial correlation of *LGR5* expression with ISC markers in GAs.

To confirm the RT-PCR results that indicated an association between *LGR5* expression and the expression of other ISC markers, we performed RNA *in situ* hybridization on GAs with basal or diffuse patterns. For a GA with a diffuse pattern, we selected one with strong and diffuse *LGR5* expression for improved visualization at a low power view. The expression of *OLFM4*, *EPHB2*, and *ASCL2* was relatively restricted to the basal region of tumor glands in the GA with basal *LGR5* expression (Fig.13A), but the expression of these markers was diffuse in the GA with a diffuse *LGR5* expression pattern (Fig. 13B). Notably, in the GA with a basal pattern, *LGR5* expression was confined to the very lower area of the tumor glands when other stem cell markers were expressed by a larger population of cells beyond the base (Fig. 13A), suggesting that *LGR5* is a most specific group of cells with stem cell features. On the other hand, for the GA with diffuse *LGR5* expression in which the majority of tumor cells expressed ISC markers as well, it remains unclear whether all *LGR5*$^{+}$ cells are tumor stem cells.

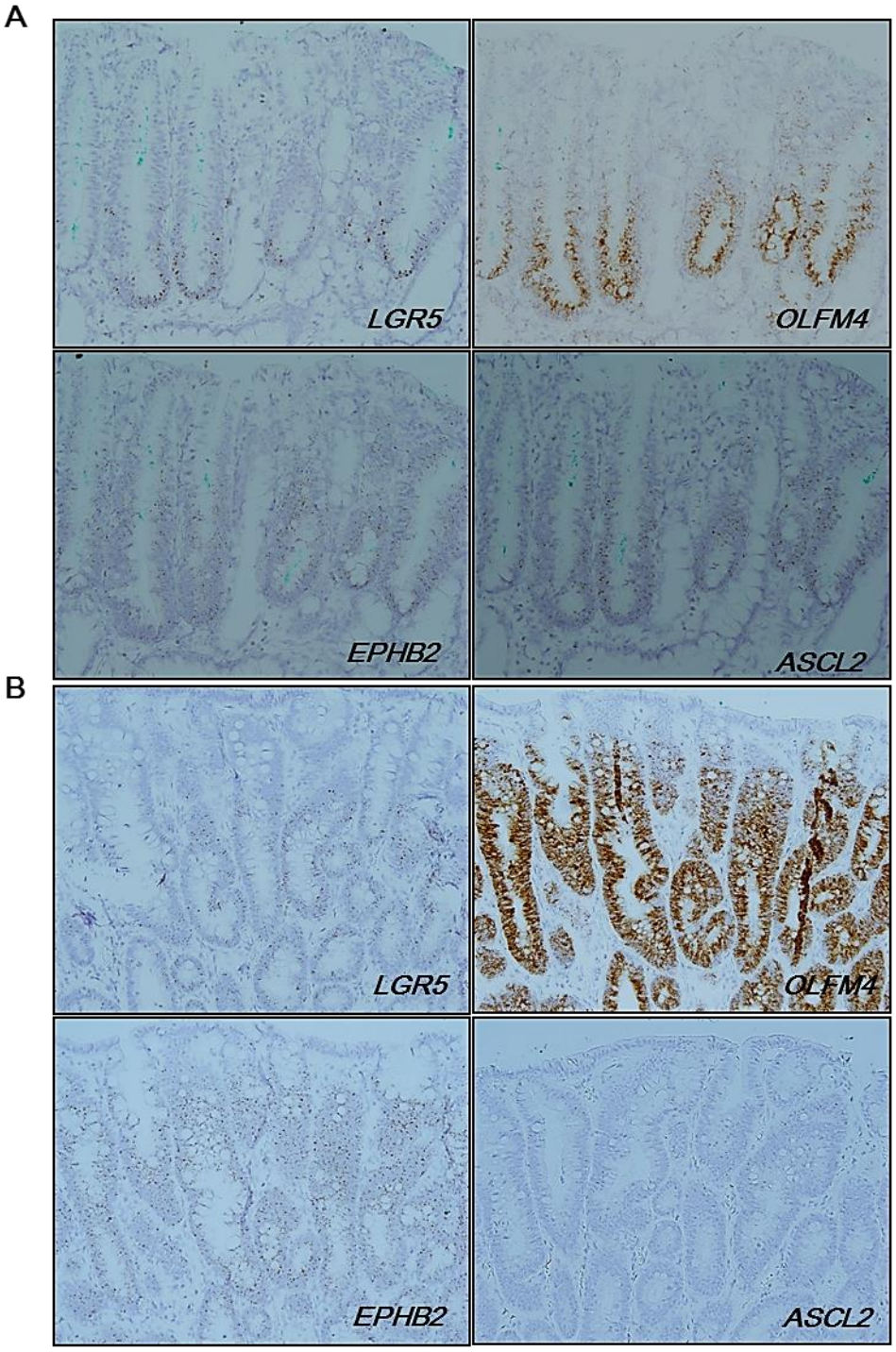
A
LGR5
OLFM4
EPHB2
ASCL2
B
LGR5
OLFM4
EPHB2
ASCL2

Figure 13. Spatial correlation of *LGR5* expression with intestinal stem cell markers in a gastric adenoma with basally distributed *LGR5*$^{+}$ cells. *OLFM4*, *EPHB2*, and *ASCL2* expressions tend to gradually increase along the axis of tumor glands in a gastric adenoma in which *LGR5* $^{+}$ cells are restricted at the base of tumor. Original magnification: A, B ×100.

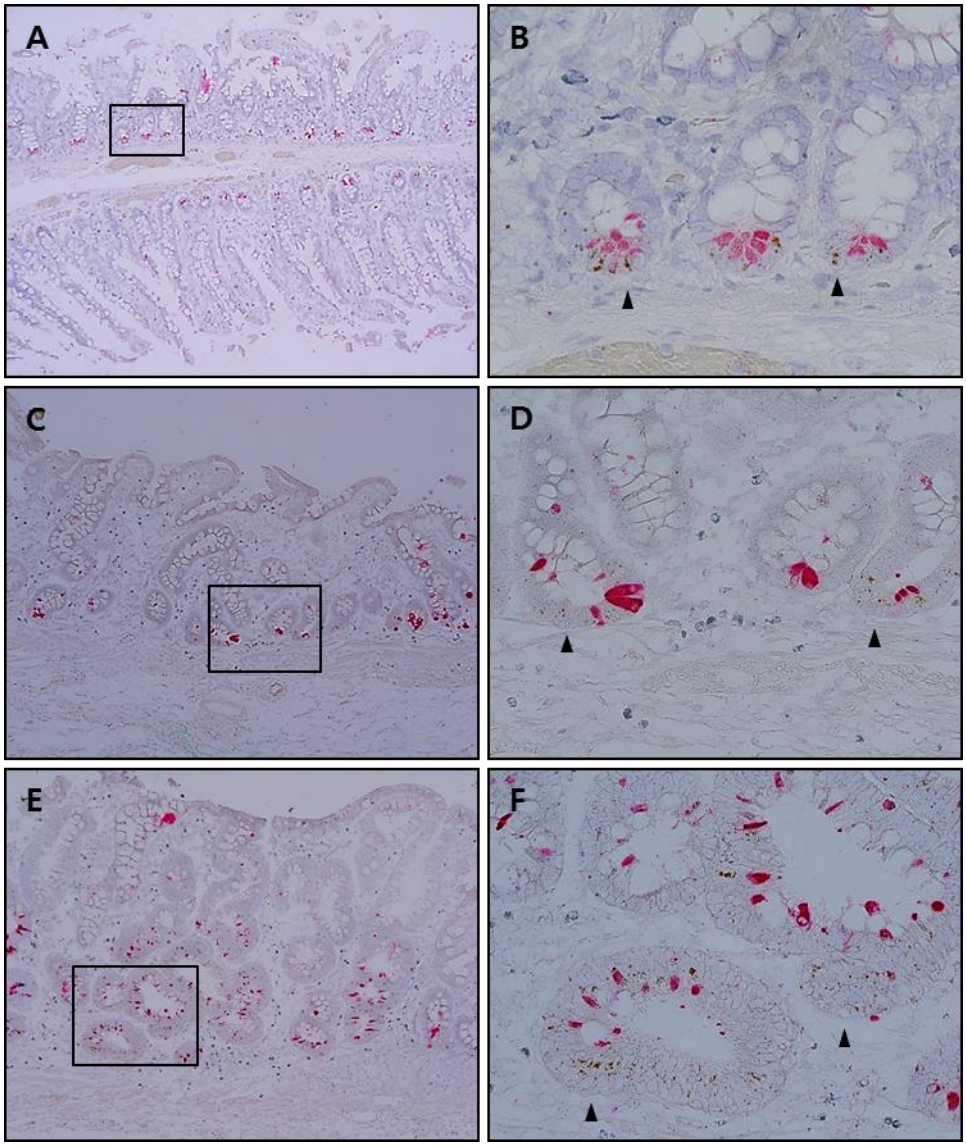

Figure 14. Spatial relationship of *LGR5*$^{+}$ cells with regard to Paneth cells. To analyze the association of *LGR5*$^{+}$ cells with Paneth cells, we performed combined RNA ISH and IHC. *LGR5*$^{+}$ cells are marked with brown dots and Paneth cells are indicated by α-defensin stain as red in the cytoplasm. (A, B) In the small intestine, *LGR5*$^{+}$ cells are always adjacent to Paneth cells

at the base of crypts. (C and D) However, some *LGR5*$^{+}$ cells that appear in the IM are not located near Paneth cells. (E and F) *LGR5*$^{+}$ gastric adenoma cells tend to locate in the tumor regardless of adenoma Paneth cells. Boxed area in figure A, C, and E is shown at higher magnification in figure B, D, and F respectively. *LGR5*$^{+}$ cells are marked by arrow heads. Original magnification: A, C, and E ×100; B, D, F ×400

Reduced *LGR5* expression in gastric cancers.

Thirty five pairs of fresh-frozen human gastric cancer tissues and matched adjacent non-tumorous gastric mucosa were collected from the patients that have undergone surgical resection, and expressions of intestinal stem cell markers including *LGR5*, *ASCL2*, *OLFM4*, and *EPHB2* were determined by RT-PCR (Fig. 15A). Contrary to gastric adenomas, gastric carcinomas revealed lower levels of *LGR5* expression than non-tumorous gastric mucosa (Fig. 15B). When dividing the cancers into either *LGR5* low and high groups by the value of 0.1 (relative mRNA level of *LGR5* to GAPDH), EPHB2 expression only was shown to be positively correlated with *LGR5* expression (Fig. 15C), but not OLFM4 and ASCL2 (Fig.15D and E).

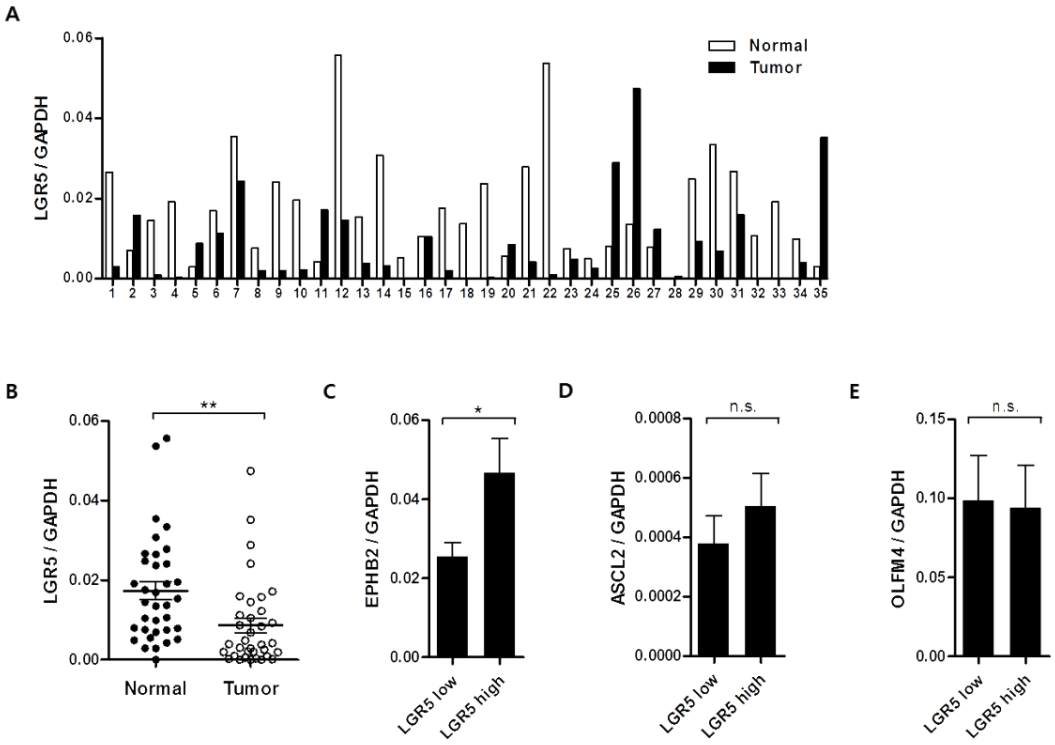

Figure 15. Correlation of *LGR5* expression with other intestinal stem cell markers in advanced gastric cancers. Expression of ISC markers including *LGR5* was examined with 35 pairs of gastric cancers and adjacent non-tumorous gastric mucosa. *LGR5* levels of gastric cancers were significantly lower than those of non-tumorous gastric tissues (B), and associated with EPHB2 expression (C), but not with OLFM4 (D) and ASCL2 expressions (E).

LGR5 is associated with poor survival in gastric cancer patients with nuclear β-catenin.

RNA ISH for *LGR5* was carried out on the tissue microarrays containing 840 gastric cancers and finally 603 cases were available for the evaluation. *LGR5* expression was scored into four categories; score 0, 1, 2, and 3, and gastric cancers with score 0 are considered as negative, gastric cancers with s 1, 2, and 3 as positive (Fig. 16). *LGR5* positivity was positively correlated with old age, well-differentiated histological type, and nuclear β-catenin expression (Table 4). Kaplan-Meier analysis revealed that *LGR5* has no prognostic significance for all the GC patients (Fig. 17A). However, for the gastric cancers with nuclear β-catenin expression, an indicator of abnormal Wnt pathway activation, *LGR5* positive-GC patients showed worse clinical outcomes than *LGR5*-negative GC patients (Fig. 17B), suggesting LGR5 as a poor prognostic marker in GCs with abnormally enhanced Wnt pathway.

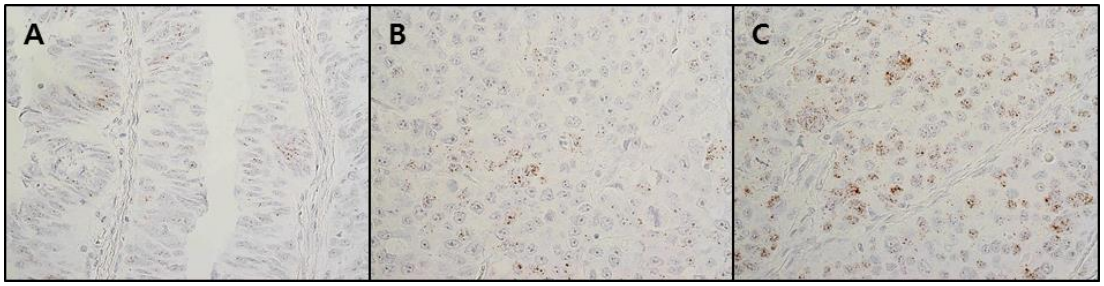

Figure 16. RNA ISH for *LGR5* in gastric carcinomas from the gastrectomy specimens. Score 0, Score 1 (A), Score 2 (B), and Score 3 (C). Original magnification: A, B, C ×400.

Table 4. Assessment of LGR5 expression in gastric carcinomas from gastrectomy specimens.

	Total (%)	LGR5		*p*-value
		Negative (%)	Positive (%)	
Patients	603	561 (93)	42 (7)	
Age				
≥65	224 (37)	199 (89)	25 (11)	0.002†
<65	379 (63)	362 (96)	17 (4)	
Gender				
Female	173 (29)	162 (94)	11 (6)	0.710†
Male	430 (71)	399 (93)	31 (7)	
Histological				
Well	125 (21)	108 (86)	17 (14)	
Moderate	240 (40)	223 (93)	17 (7)	
Poor	147 (24)	143 (97)	4 (3)	
Signet ring cell	62 (10)	60 (97)	2 (3)	0.0260†
Mucinous	7 (1)	7 (100)	0 (0)	
Papillary	15 (3)	13 (87)	2 (13)	
Others	7 (1)	7 (100)	0 (0)	
Lymphatic invasion				
Negative	216 (36)	205 (95)	11 (5)	0.1770†
Positive	387 (64)	356 (92)	31 (8)	
Venous invasion				
Negative	499 (83)	468 (94)	31 (6)	0.1590†
Positive	104 (17)	93 (89)	11 (11)	
TNM_7th				
I	167 (27)	155 (93)	12 (7)	
II	163 (27)	147 (90)	16 (10)	
III	213 (35)	198 (93)	15 (7)	0.1590†
IV	66 (11)	61 (92)	5 (8)	
β-catenin				
Nuclear stain	34 (6)	23 (68)	11 (32)	0.000†
No nuclear stain	569 (94)	538 (95)	31 (5)	

†Fisher's exact test.

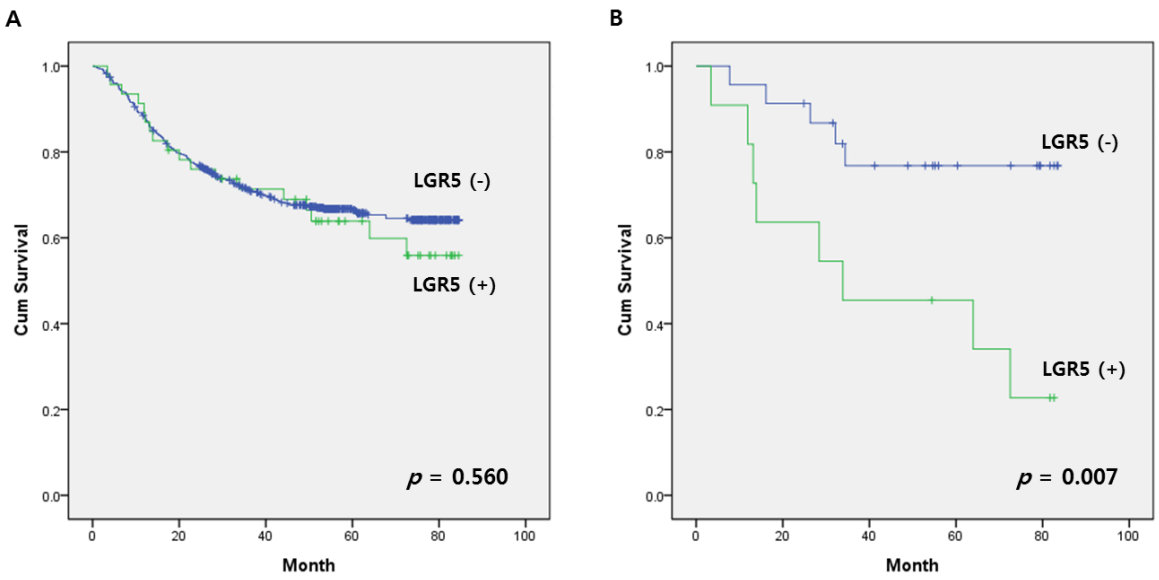

Figure 17. Survival rate of gastric cancer patients with *LGR5* expression.

Kaplan-Meier analysis demonstrated that *LGR5* positivity has no prognostic influence in gastric cancer patients. However, for the gastric cancers with nuclear β-catenin expression, *LGR5* expression was associated with poor clinical outcomes.

No effects of *LGR5* expression on the growth of gastric cancer cells.

As *LGR5* positivity showed worse prognosis for the GC patients with nuclear β-catenin, we decided to examine the functional significance of *LGR5* on cancer cell growth. *LGR5* expression was examined in fifteen GC cell lines (Fig. 18A), and which were divided into *LGR5*-high and -low groups. *LGR5*-high group exhibited slightly higher levels of *ASCL2* than *LGR5*-low group (Fig. 18B). Three GC cell lines including SNU719, MKN28, and MKN74 were chosen since they showed low levels of endogenous *LGR5* and nuclear β−catenin expression (Fig. 18C). *LGR5* overexpression was induced by transfection of *LGR5* in each cell lines, which was confirmed by RT-PCR (Fig. 19A) and western blot (Fig. 19B). Relative growth rate was measured 3 or 4 days after transfection. There was no difference in the proliferation between cancer cells transfected with *LGR5* and control vector (Figure 19C). Even treatment with R-spondin 1 (500ng/ml), a ligand for LGR5 showed no influence on the proliferation of cancer cells (Fig. 19D). Wound healing assay showed that *LGR5* expression had no impact on the migration activity of gastric cancer cells neither (Fig. 20).

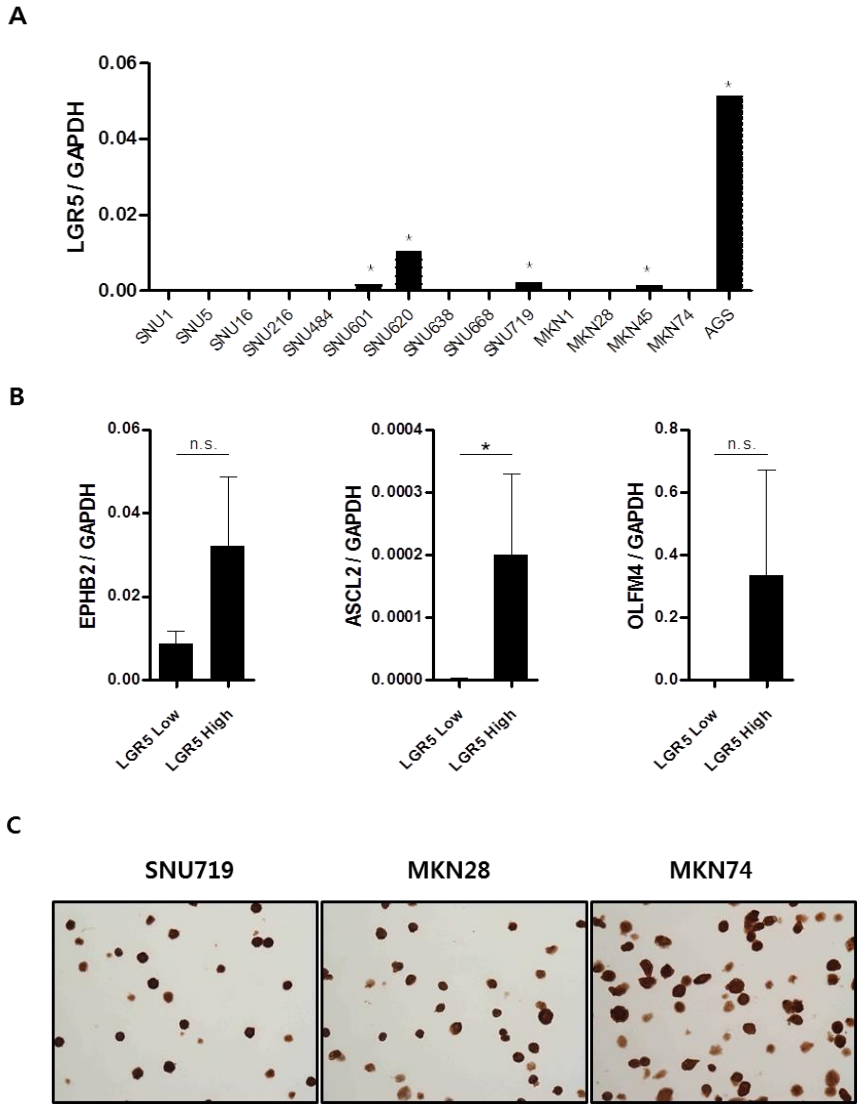

Figure 18. Expression of *LGR5* in the gastric cancer (GC) cell lines. (A) Fifteen GC cell lines were examined to determine the levels of endogenous *LGR5*, and five of them showed relatively higher *LGR5* expression than the other 10 GC cell lines. Asterisks indicate a group of *LGR5*-high cell lines. (B) GC cell lines with high *LGR5* were demonstrated to have higher levels of ASCL2 than those with low *LGR5*. (C) Three cell lines, SNU719, MKN28, and MKN74 are positive for nuclear β-catenin.

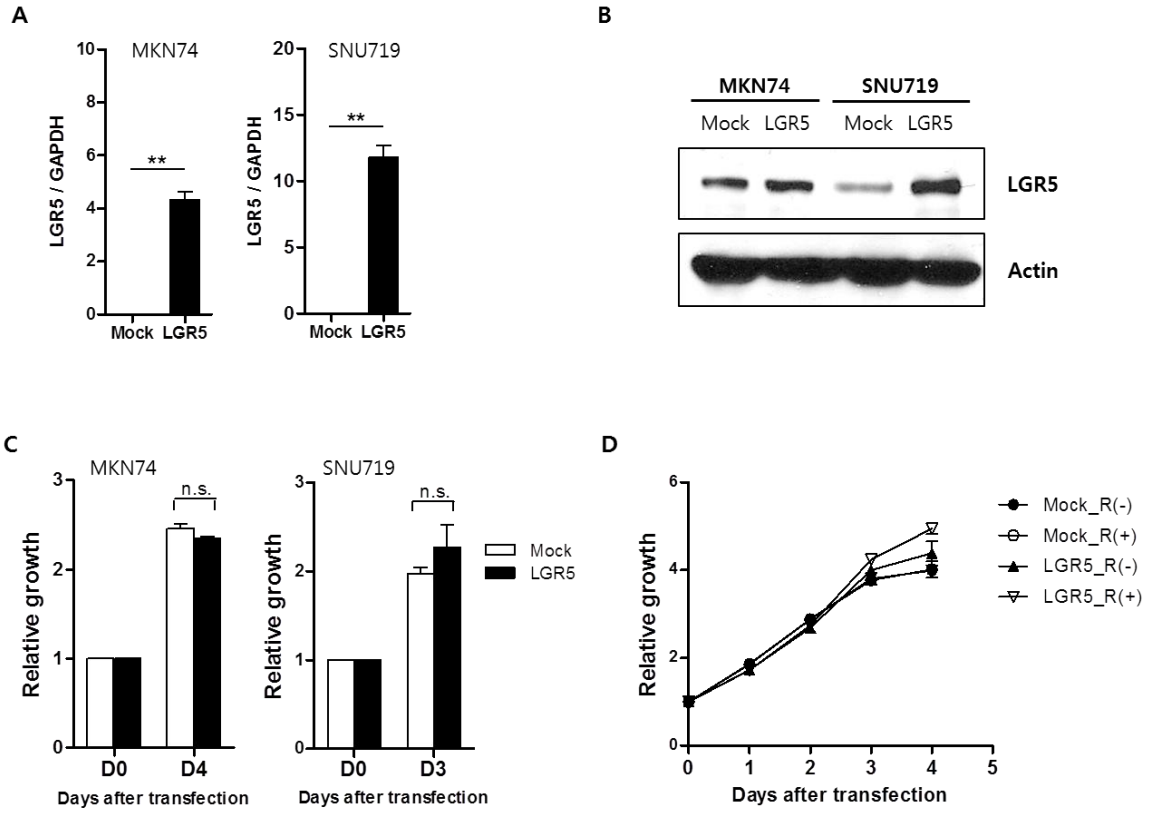

Figure 19. Effects of *LGR5* expression on the growth of gastric cancer cell lines. *LGR5* overexpression induced by transfection of *LGR5* into two gastric cancer cell lines, MKN28 and SNU719 was confirmed by RT-PCR (A) and Western blot (B). (C) There was no difference in the growth rate between the cancer cells with and without *LGR*5 overexpression. (D) Treatment with R-spondin 1 (500ng/ml), a ligand for LGR5, had no influence on the proliferation of MKN28 cells either. R, R-spondin 1.

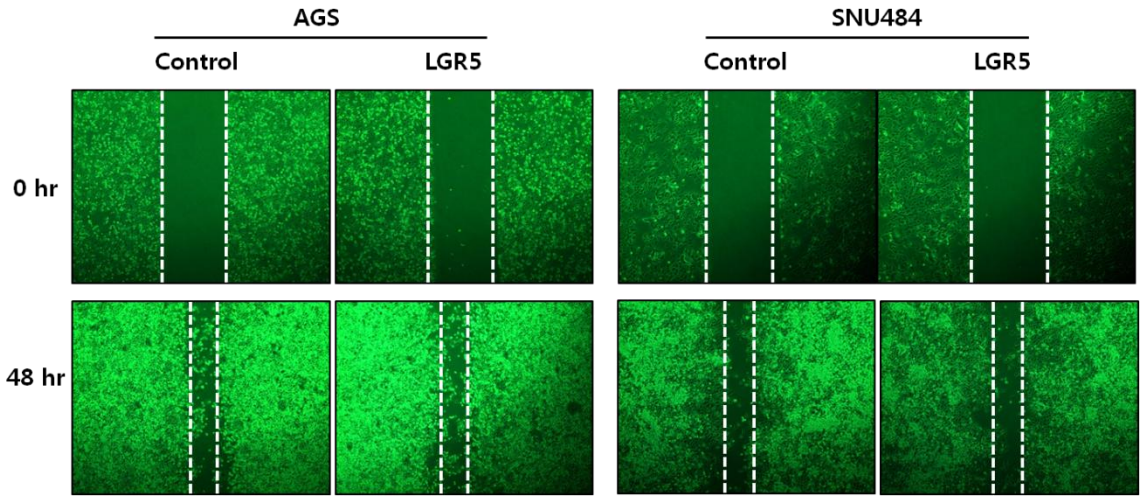

Figure 20. Effects of *LGR5* expression on migration capacity of gastric cancer cell lines. *LGR5* expression was induced in two gastric cancer cell lines, AGS and SNU484. A migration was evaluated by wound healing assay, which showed that there was no difference in migration activity between control and *LGR5* expression groups at 48 hours after scratching.

DISCUSSION

Growing evidence supports that *Lgr5* is a normal gastrointestinal tract stem cell marker in mice, with a corresponding role in murine tumors. Investigations of *LGR5* expression in human tissues, however, have been limited, and an appropriate histological method to identify *LGR5*$^{+}$ cells in human organs has not been established. Previous studies that attempted to use antibodies or RNA ISH on human FFPE tissues did not seem to provide accurate results with regard to the specific labeling of *LGR5*$^{+}$ cells (10-15). For example, Uehara et al. (29) and Wu et al. (30) recently reported the distribution of *LGR5* cells in human gastric glands using commercially available *LGR5* antibodies. However, an appropriate positive control stain to validate the specificity of the antibodies was not provided, and the results showed nonspecific staining of parietal cells or hematopoietic cells in the lamina propria of the stomach. Simon et al. generated monoclonal antibodies to *LGR5* to investigate the histo-anatomical distribution of *LGR5*$^{+}$ cells with gastric cancer progression and validated its specificity by western blot analysis of *LGR5*-transfected cell lines (11). However, the immunostaining of colonic mucosa as a positive control was not entirely convincing because of the strong positive staining of stromal and endothelial cells. More importantly, none of these studies demonstrated the specific localization of *LGR5* cells at the basal glands of normal gastric antrum, as shown in mice. Nakata et al. (31) and Becker et al. (12) did provide a positive control stain for *LGR5* antibodies with the intestinal mucosa before using the antibodies in brain and colonic

tumors, but the quality of the staining was not sufficient to ensure the sensitivity and specificity of the antibodies. Although RNA ISH has specifically shown the *LGR5*$^{+}$ cells restricted at the crypt base in studies of human and murine intestines, the visualization quality of *LGR5*$^{+}$ cells in FFPE tissues was not satisfying, and the technique has not been used in human gastric tissues (14, 15, 32).

In the present study, we used RNAscope to determine the presence of *LGR5*$^{+}$ cells in various gastric lesions after validating the technique. We specifically identified *LGR5*$^{+}$ cells at the same locations in human gastric mucosa, intestines, and hair follicles as previously shown in mice. Moreover, the quality of the staining was much better than conventional RNA ISH, which made it easier to evaluate *LGR5*$^{+}$ cells in their cellular context. Consequently, we expect that this method will facilitate studies of *LGR5*$^{+}$ cells in other archived human samples, which could in turn accelerate investigations into the practical significance of *LGR5* in a variety of human diseases. However, RNA ISH only detects cells that contain *LGR5* transcripts; it is unknown whether *LGR5* transcripts are sufficiently translated into proteins that play functional roles in determining stem cell properties. It remains a possibility that *LGR5* serves mainly as a surrogate stem cell marker without any functional implications. Although *LGR5* acts as a receptor for ligands such as R-spondins and helps augment Wnt signaling (33, 34), the functional relevance of *LGR5* in humans with regard to stem cell activity has yet to be determined.

We observed *LGR5*$^+$ cells at almost all crypts of the small intestine and colon and at the hair follicle bulges, which confirmed that *LGR5*$^+$ cells are a major stem cell population in these tissues. However, *LGR5*$^+$ cells were barely detectable in the antral glands of the normal gastric mucosa, suggesting that *LGR5*$^+$ cells in the stomach comprise only a small fraction of the total stem cell population. The stomach can be divided into 4 major parts, depending on its histo-anatomical features, and all proposed stem cell markers to date are present in a limited area of the stomach (35). Therefore, the stomach likely contains many heterogeneous stem cell populations with distinct characteristics and different markers. The intestinal epithelium is also believed to contain 2 distinct pools of stem cells, the *Bmi1*-expressing +4 cells and the *LGR5*$^+$ crypt-based columnar cells (36).

LGR5$^+$ cells in the normal antral glands were sparse and unaffected by inflammation or *Helicobacter pylori* infection. In contrast, the number of *LGR5*$^+$ cells and the staining intensity were remarkably increased in IM to nearly the same levels observed in the small intestine. Interestingly, *LGR5*$^+$ cells also appeared in IM of the fundic glands, in which *LGR5*$^+$ cells are normally absent, implying that intestinalized gastric epithelial cells, including the *LGR5*$^+$ cells in IM, might not arise from the existing *LGR5*$^+$ stem cells. Indeed, spasmolytic polypeptide-expressing metaplasia (SPEM), another type of stomach metaplasia, has been shown to not arise from *LGR5*$^+$ cells (37), but transdifferentiates from mature chief cells in the murine (38) and human (39,

40) stomach. Moreover, *LGR5*$^{+}$ stem cells arise from *Bmi-1*-expressing stem cells in the intestinal epithelium (36). Collectively, these findings suggest that the *LGR5*$^{+}$ cell expansion in IM arises from another group of stem cells, although no stem cell population is yet known to generate *LGR5*$^{+}$ cells in the stomach.

Intestinalized gastric glands are similar in many aspects to the small intestinal epithelium. However, IM is not identical to the intestinal mucosa. One significant difference is that Paneth cells are less frequently found in IM. Paneth cells may be essential for the maintenance of *LGR5*$^{+}$ stem cells in intestinal crypts (41). However, in IM, *LGR5*$^{+}$ cells usually exist in the absence of Paneth cells, indicating that *LGR5*$^{+}$ cells in IM do not rely on Paneth cells as a source of signaling factors, such as Wnt ligands, Notch ligands, and epidermal growth factor, for survival. Even when Paneth cells are present in IM and GAs, *LGR5*$^{+}$ cells are not necessarily located next to Paneth cells (Fig. 14). Instead of Paneth cells, *LGR5*$^{+}$ cells have redundant sources of survival signals. For instance, Wnt ligands from mesenchymal cells can compensate for the loss of signals from Paneth cells (42), and c-kit^{+} secretory cells have been identified as a colonic counterpart of Paneth cells that could support *LGR5*$^{+}$ stem cells (43). Additionally, it was recently shown that Paneth cells are not required to sustain *LGR5*$^{+}$ cells *in vivo* (44). Thus, *LGR5*$^{+}$ stem cells in IM might be maintained by an undefined epithelial or mesenchymal cell population that substitutes for Paneth cells.

We speculate that the marked increase in the number of *LGR5*$^+$ cells during the process of IM has profound biological significance for tumor initiation in the stomach. A study of *Cdx2*-transgenic mice demonstrated that IM plays a significant role in the genesis of gastric carcinoma and that the cancer cells originated from intestinal metaplastic epithelial cells that had been entirely transformed from gastric cells by Cdx2 (45). In addition, an increased number of *LGR5*$^+$ cells were observed in the normal intestinal tissues of *Apc* mutant mice and proposed as the cause of more severe polyposis (14). Accordingly, given that *LGR5*$^+$ cells are the cells of origin of Wnt-driven tumors in the murine stomach (9), the expanded pool of *LGR5*$^+$ stem cells might be one of the major factors of IM that contributes to tumor development in the human stomach. However, because a lineage tracing study is not applicable for human tissues at this time, direct evidence that human GAs derive from *LGR5*$^+$ cells cannot be obtained. Therefore, future studies on the relationship of *LGR5*$^+$ cells and GA development are required.

LGR5$^+$ cells were present in human GAs, where they accounted for 0 to >90% of the tumor cells with 2 main distribution patterns. In addition to tumors with a basally restricted pattern of *LGR5*$^+$ cells, we also observed adenomas with *LGR5*$^+$ cells that were dispersed throughout the tumor mass; this was not noted in a mouse study, in which approximately 5–10% of the tumor cells in most of the intestinal adenomas were *LGR5*$^+$ cells, which were mainly located at the basal areas of the tumor glands (7). This was probably because the intestinal adenomas in the mice all arose from the same *Apc* mutation,

whereas human adenomas develop in response to many different types of Wnt-pathway abnormalities, likely in combination with other genetic abnormalities, which results in tumors with different levels of Wnt signaling and varying numbers of *LGR5*$^{+}$ cells. In fact, the level of *LGR5* expression in adenomas of 2 intestinal tumorigenesis mouse models, *Apc*^{1322T} (1322T) and *Apc*^{R850X} (Min), differed: 1322T tumors had higher *LGR5* expression levels than Min tumors, and more than half of the epithelial portion of the adenomas showed *LGR5* expression (14). Therefore, in GAs, both the distribution pattern and the number of *LGR5*$^{+}$ cells are likely to differ according to the degree of Wnt pathway activation.

In most of the low-grade adenomas, at least 5% of the tumor cells were *LGR5*$^{+}$ cells. We might consider *LGR5*$^{+}$ cells in the niches of normal tissues as stem cells; however, *LGR5*$^{+}$ cells within a tumor mass do not necessarily serve as tumor stem cells. EPHB2- and *LGR5*-enriched cells reportedly comprise a stem-like cell population in human colorectal cancers (28). However, it has not been evaluated whether *LGR5*$^{+}$ cells in human gastric tumors retain stem cell properties. To investigate whether *LGR5*$^{+}$ cells in gastric tumors had any stem cell features, we selected GAs with basally restricted *LGR5*$^{+}$ cells that were reminiscent of the normal crypt and IM, and then divided the tumor glands into upper and lower regions by laser capture microdissection. Our study demonstrated that the basal regions of tumor glands, which have a majority of the *LGR5*$^{+}$ cells, express significantly higher levels of ISC markers and *CD133* than the upper region. In contrast, the

differential expression of ISC markers was substantially attenuated in GAs with diffusely distributed *LGR5*$^{+}$ cells, which was confirmed by the co-localization of *LGR5* and ISC markers in RNA *in situ* hybridization. These findings indicate that *LGR5* expression is closely linked to increased expression of ISC markers and provide compelling evidence that basally restricted *LGR5*$^{+}$ cells in GAs act as stem cells. However, the question remains whether the *LGR5*$^{+}$ cells that are distributed diffusely across the adenoma and co-express ISC markers also have stem cell features; they seem too numerous to be stem cells and lack the spatial restriction to the base of the glands. If the diffuse expression only derives from strong Wnt pathway activation, as we mentioned earlier, *LGR5* may not be appropriate for use as a stem cell marker.

Contrary to the high levels of *LGR5* in GAs, *LGR5* expression in gastric carcinomas (GCs) was even lower than that in normal gastric mucosa, and its positive correlation with other ISC markers was found only with EPHB2 but not with OLFM4 and ASCL2. According to the colon cancer model with regard to *Lgr5*, the gradual accumulation of additional mutations within *Lgr5*-expressing tumor stem cells drives cancer progression over time (46). Therefore, given the histological difference between GAs and GCs; uniform tumor cells of GAs and remarkable heterogeneity of gastric cancer cells, this reduced expression of *LGR5* in GCs could be explained by the emergence of more aggressive clones within the tumor masses. Although it has been suggested that *LGR5* positive cells act as stem cells in the colon cancers, there

is no evidence so far that *LGR5* cells function as stem cells in gastric cancers. In addition, we could not find any significant growth benefit when *LGR5* expression was induced in gastric cancer cells in vitro. Also, the effects of *LGR5* on the growth of colon cancer cells are not consistent (47, 48). Further study is demanded to unravel the biological implications of *LGR5* in advanced gastric cancers, thereby we will be able to explore the potential of *LGR5* as a candidate marker for the targeted therapy of gastric cancers.

REFERENCES

1. Visvader JE, Lindeman GJ. Cancer stem cells in solid tumours: accumulating evidence and unresolved questions. Nature reviews Cancer. 2008 Oct;8(10):755-68.

2. Wicha MS, Liu S, Dontu G. Cancer stem cells: an old idea--a paradigm shift. Cancer research. 2006 Feb 15;66(4):1883-90; discussion 95-6. .

3. Barker N, van Es JH, Kuipers J, Kujala P, van den Born M, Cozijnsen M, et al. Identification of stem cells in small intestine and colon by marker gene *LGR5*. Nature. 2007 Oct 25;449(7165):1003-7.

4. Yan KS, Chia LA, Li X, Ootani A, Su J, Lee JY, et al. The intestinal stem cell markers Bmi1 and *LGR5* identify two functionally distinct populations. Proceedings of the National Academy of Sciences of the United States of America. 2012 Jan 10;109(2):466-71.

5. Snippert HJ, van Es JH, van den Born M, Begthel H, Stange DE, Barker N, et al. Prominin-1/CD133 marks stem cells and early progenitors in mouse small intestine. Gastroenterology. 2009 Jun;136(7):2187-94.

6. Barker N, Ridgway RA, van Es JH, van de Wetering M, Begthel H, van den Born M, et al. Crypt stem cells as the cells-of-origin of intestinal cancer. Nature. 2009 Jan 29;457(7229):608-11.

7. Schepers AG, Snippert HJ, Stange DE, van den Born M, van Es JH, van de Wetering M, et al. Lineage tracing reveals *LGR5*+ stem cell activity in mouse intestinal adenomas. Science. 2012 Aug 10;337(6095):730-5.

8. Leushacke M, Barker N. *LGR5* and Lgr6 as markers to study adult stem cell roles in self-renewal and cancer. Oncogene. 2012 Jun 21;31(25):3009-22.

9. Barker N, Huch M, Kujala P, van de Wetering M, Snippert HJ, van Es JH, et al. *LGR5*(+ve) stem cells drive self-renewal in the stomach and build long-lived gastric units in vitro. Cell stem cell. 2010 Jan 8;6(1):25-36.

10. von Rahden BH, Kircher S, Lazariotou M, Reiber C, Stuermer L, Otto C, et al. *LGR5* expression and cancer stem cell hypothesis: clue to define the true origin of esophageal adenocarcinomas with and without Barrett's esophagus? Journal of experimental & clinical cancer research : CR. 2011;30:23.

11. Simon E, Petke D, Boger C, Behrens HM, Warneke V, Ebert M, et al. The spatial distribution of *LGR5*+ cells correlates with gastric cancer progression. PloS one. 2012;7(4):e35486.

12. Becker L, Huang Q, Mashimo H. Immunostaining of *LGR5*, an intestinal stem cell marker, in normal and premalignant human gastrointestinal tissue. TheScientificWorldJournal. 2008;8:1168-76.

13. Wang T, Yeoh KG, Salto-Tellez M. *LGR5* expression is absent in human premalignant lesions of the stomach. Gut. 2012 Mar 22.

14. Lewis A, Segditsas S, Deheragoda M, Pollard P, Jeffery R, Nye E, et al. Severe polyposis in Apc(1322T) mice is associated with submaximal Wnt signalling and increased expression of the stem cell marker *LGR5*. Gut. 2010 Dec;59(12):1680-6.

15. Uchida H, Yamazaki K, Fukuma M, Yamada T, Hayashida T, Hasegawa H, et al. Overexpression of leucine-rich repeat-containing G protein-coupled receptor 5 in colorectal cancer. Cancer science. 2010 Jul;101(7):1731-7.

16. Wakatsuki K, Yamada Y, Narikiyo M, Ueno M, Takayama T, Tamaki H, et al. Clinicopathological and prognostic significance of mucin phenotype in gastric cancer. Journal of surgical oncology. 2008 Aug 1;98(2):124-9.

17. Namikawa T, Hanazaki K. Mucin phenotype of gastric cancer and clinicopathology of gastric-type differentiated adenocarcinoma. World journal of gastroenterology : WJG. 2010 Oct 7;16(37):4634-9.

18. Bonin S, Hlubek F, Benhattar J, Denkert C, Dietel M, Fernandez PL, et al. Multicentre validation study of nucleic acids extraction from FFPE tissues. Virchows Archiv : an international journal of pathology. 2010 Sep;457(3):309-17.

19. Jaks V, Barker N, Kasper M, van Es JH, Snippert HJ, Clevers H, et al. *LGR5* marks cycling, yet long-lived, hair follicle stem cells. Nat Genet. 2008;40(11):1291-9.

20. Wang F, Flanagan J, Su N, Wang LC, Bui S, Nielson A, et al. RNAscope: a novel in situ RNA analysis platform for formalin-fixed, paraffin-embedded tissues. The Journal of molecular diagnostics : JMD. 2012 Jan;14(1):22-9.

21. Tanese K, Fukuma M, Yamada T, Mori T, Yoshikawa T, Watanabe W, et al. G-protein-coupled receptor GPR49 is up-regulated in basal cell carcinoma and promotes cell proliferation and tumor formation. The American journal of pathology. 2008 Sep;173(3):835-43.

22. Yuasa Y. Control of gut differentiation and intestinal-type gastric carcinogenesis. Nature reviews Cancer. 2003 Aug;3(8):592-600.

23. Mizrak D, Brittan M, Alison M. CD133: molecule of the moment. The Journal of pathology. 2008 Jan;214(1):3-9.

24. Abraham SC, Montgomery EA, Singh VK, Yardley JH, Wu TT. Gastric adenomas: intestinal-type and gastric-type adenomas differ in the risk of adenocarcinoma and presence of background mucosal pathology. The American journal of surgical pathology. 2002 Oct;26(10):1276-85.

25. Lee JH, Abraham SC, Kim HS, Nam JH, Choi C, Lee MC, et al. Inverse relationship between APC gene mutation in gastric adenomas and development of adenocarcinoma. The American journal of pathology. 2002 Aug;161(2):611-8.

26. Takahashi H, Ishii H, Nishida N, Takemasa I, Mizushima T, Ikeda M, et al. Significance of *LGR5*(+ve) cancer stem cells in the colon and rectum. Annals of surgical oncology. 2011 Apr;18(4):1166-74.

27. Fan XS, Wu HY, Yu HP, Zhou Q, Zhang YF, Huang Q. Expression of *LGR5* in human colorectal carcinogenesis and its potential correlation with beta-catenin. International journal of colorectal disease. 2010 May;25(5):583-90.

28. Merlos-Suarez A, Barriga FM, Jung P, Iglesias M, Cespedes MV, Rossell D, et al. The intestinal stem cell signature identifies colorectal cancer stem cells and predicts disease relapse. Cell stem cell. 2011 May 6;8(5):511-24.

29. Uehara T, Ma D, Yao Y, Lynch JP, Morales K, Ziober A, et al. H. pylori infection is associated with DNA damage of *LGR5*-positive epithelial stem cells in the stomach of patients with gastric cancer. Digestive diseases and sciences. 2013 Jan;58(1):140-9.

30 Wu C, Xie Y, Gao F, Wang Y, Guo Y, Tian H, et al. *LGR5* expression as stem cell marker in human gastric gland and its relatedness with other putative cancer stem cell markers. Gene. 2013 Aug 1;525(1):18-25.

31. Nakata S, Campos B, Bageritz J, Bermejo JL, Becker N, Engel F, et al. *LGR5* is a marker of poor prognosis in glioblastoma and is required for survival of brain cancer stem-like cells. Brain pathology. 2013 Jan;23(1):60-72.

32. Leedham SJ, Rodenas-Cuadrado P, Howarth K, Lewis A, Mallappa S, Segditsas S, et al. A basal gradient of Wnt and stem-cell number influences regional tumour distribution in human and mouse intestinal tracts. Gut. 2013 Jan;62(1):83-93.

33. Carmon KS, Gong X, Lin Q, Thomas A, Liu Q. R-spondins function as ligands of the orphan receptors LGR4 and *LGR5* to regulate Wnt/beta-catenin signaling. Proceedings of the National Academy of Sciences of the United States of America. 2011 Jul 12;108(28):11452-7.

34. Ruffner H, Sprunger J, Charlat O, Leighton-Davies J, Grosshans B, Salathe A, et al. R-Spondin potentiates Wnt/beta-catenin signaling through orphan receptors LGR4 and *LGR5*. PloS one. 2012;7(7):e40976.

35. Qiao XT, Gumucio DL. Current molecular markers for gastric progenitor cells and gastric cancer stem cells. Journal of gastroenterology. 2011 Jul;46(7):855-65.

36 Tian H, Biehs B, Warming S, Leong KG, Rangell L, Klein OD, et al. A reserve stem cell population in small intestine renders *LGR5*-positive cells dispensable. Nature. 2011 Oct 13;478(7368):255-9.

37. Nam KT, O'Neal RL, Coffey RJ, Finke PE, Barker N, Goldenring JR. Spasmolytic polypeptide-expressing metaplasia (SPEM) in the gastric oxyntic mucosa does not arise from *LGR5*-expressing cells. Gut. 2011 Dec 23.

38. Nam KT, Lee HJ, Sousa JF, Weis VG, O'Neal RL, Finke PE, et al. Mature chief cells are cryptic progenitors for metaplasia in the stomach. Gastroenterology. 2010 Dec;139(6):2028-37.

39. Lennerz JK, Kim SH, Oates EL, Huh WJ, Doherty JM, Tian X, et al. The transcription factor MIST1 is a novel human gastric chief cell marker whose expression is lost in metaplasia, dysplasia, and carcinoma. The American journal of pathology. 2010 Sep;177(3):1514-33.

40. Capoccia BJ, Jin RU, Kong YY, Peek RM, Jr., Fassan M, Rugge M, et al. The ubiquitin ligase Mindbomb 1 coordinates gastrointestinal secretory cell maturation. The Journal of clinical investigation. 2013 Apr 1;123(4):1475-91. PubMed PMID: 23478405.

41. Sato T, van Es JH, Snippert HJ, Stange DE, Vries RG, van den Born M, et al. Paneth cells constitute the niche for *LGR5* stem cells in intestinal crypts. Nature. 2011 Jan 20;469(7330):415-8.

42. Farin HF, Van Es JH, Clevers H. Redundant sources of Wnt regulate intestinal stem cells and promote formation of Paneth cells. Gastroenterology. 2012 Dec;143(6):1518-29 e7.

43. Rothenberg ME, Nusse Y, Kalisky T, Lee JJ, Dalerba P, Scheeren F, et al. Identification of a cKit(+) colonic crypt base secretory cell that supports *LGR5*(+) stem cells in mice. Gastroenterology. 2012 May;142(5):1195-205.

44. Kim TH, Escudero S, Shivdasani RA. Intact function of *LGR5* receptor-expressing intestinal stem cells in the absence of Paneth cells. Proceedings of the National Academy of Sciences of the United States of America. 2012 Mar 6;109(10):3932-7.

45. Mutoh H, Sakurai S, Satoh K, Tamada K, Kita H, Osawa H, et al. Development of gastric carcinoma from intestinal metaplasia in Cdx2-transgenic mice. Cancer research. 2004 Nov 1;64(21):7740-7.

46. M Leushacke, N Barker. Lgr5 and Lgr66 as markers to study adult stem cell roles in self-renewal and cancer. Oncogene 2012 Jun,31(25): 3009-22

47. Whissel G, MOntagni E, Marinelli P, Hermando-Monblona X, Sevillano M, Jung P et al. The transcription factor GATA6 enables self-renewal of colon adenoma stem cells by repressing BMP gene expression. Nat Cell Biol. 204 Jul;16(7):695-707

48. Tsuji S, Kawasaki Y, Furukawa S, Taniue K, Hyashi T, Okuno M et al. The miR-363-GATA-Lgr5 pathway is critical for colorectal tumourigenesis. Nat Commun. 2014;5:3150

국문 초록

Lgr5 는 마우스 위장관 점막의 유력한 줄기세포 표지자로 알려져 있다. 또한, 계통 추적 실험을 통해 위장관에서 발생하는 종양의 기원세포이며 동시에 소위 “암 줄기세포”의 가능성이 제기되었다. 이번 연구에서는, 인간의 정상 위 점막 및 위 종양에서 *LGR5* 양성세포의 존재 및 그 분포, 그리고 종양형성에 있어서 생물학적인 의의를 밝히고자 하였다. RNAscope 이라는 새로운 RNA in situ hybridization (ISH) 기법을 활용하여 정상 위 전정부의 기저부에 *LGR5* 양성 세포가 위치하며, 장형화생이 일어난 경우 *LGR5* 발현이 급격히 증가한다는 사실을 발견하였다. 위 선종의 76%, 조기위암의 43%에서 *LGR5* 양성 종양세포를 관찰하였다. *LGR5* 발현은 저 등급 (low grade), 베타 카테닌 양성, 그리고 조직학적으로는 소장 타입(intestinal type)과 연관되어 있었고, 이러한 결과는 위 종양 발생의 초기 단계에서 *LGR5* 이 관련되어 있을 가능성을 시사하였다. 흥미로운 사실은 빈번하게 *LGR5* 양성 종양세포가 정상 조직에서와 유사하게 종양 샘의 기저부에 주로 위치하고 있었으며, 다른 위장관 줄기세포 표지자인 *OLFM4*, *EPHB2*, 그리고 *ASCL2* 의 발현과 밀접히 연관되어 있었다는 점이다. 이는 인간의 위 종양에서도 *LGR5* 양성세포가 종양줄기세포로 기능할 가능성을 보여주는 결과이다. 베타 카테닌 양성 위암 환자 군에서 *LGR5* 양성이 나쁜 예후와 관련되어 있다는 사실을 발견하였지만, 위암 세포주에 *LGR5* 를 과발

현시켰을 때 암세포의 성장에는 별다른 영향을 미치지 않아 진행성 위암에서 *LGR5* 양성 세포의 생물학적 역할에 대해서는 추가 연구가 필요할 것으로 여겨진다.

주요어 : Leucine-rich repeat-containing G-coupled Receptor 5 (LGR5), 암 줄기세포, 위선종, 위암

학 번 : 2009-30581